

Stream Flow Response due to Land Cover Change in Megech Watershed, Upper Blue Nile basin, Ethiopia



Bahir Dar University

Bahir Dar Institute of Technology

Faculty of Civil and Water Resources Engineering

Hydraulic and Water Resources Engineering

By Zemenu Addis

March, 2017

Bahir Dar, Ethiopia

Stream Flow Response Due to Land Cover Change in Megech Watershed Upper Blue Nile basin

A thesis submitted in partial fulfillment of the requirements for the Degree of Master of Science in "Water Resource Engineering" specialization in "Engineering Hydrology" Presented to the Faculty of Civil and Water Resources Engineering, Bahir Dar Institute of Technology, Bahir Dar University.

IJSER

Supervised By: Mamaru A. Moges (PhD)

March, 2016

Bahir Dar, Ethiopia

DECLARATION

I, the undersigned, hereby declare that this thesis entitled “**Stream flow response due to land cover change in Megech Watershed, upper Blue Nile Basin**” submitted for the partial fulfillment of the requirements for the Masters of Science in Engineering Hydrology, is the original work done by me under the supervision of Mamaru A. Moges and this thesis has not been published or submitted elsewhere for the requirement of a degree program to the best of my knowledge and belief. Materials or ideas of other authors used in this thesis have been duly acknowledged and references are listed at the end of the main text.

Signature

Name of the student

Date

IJSER

The thesis entitled **“Stream flow response due to land cover change in Megech Watershed, upper Blue Nile Basin in Ethiopia”** by Zemenu Addis T/Medhin is approved for the degree of Master of Science in Water Resource Engineering specialization in Engineering Hydrology.

APPROVAL SHEET

Board of Examiners

Approved by Board of Examiners

_____	_____	_____
Faculty Dean	Signature	Date
_____	_____	_____
Advisor	Signature	Date
_____	_____	_____
External Examiner	Signature	Date
_____	_____	_____
Internal Examiner	Signature	Date

Abstract

The main focus of the present study was evaluating the impacts of land cover change on the stream flow of Megech river basin. Land sat 1(1973), Land sat 5 (1986) and Land sat 8 (2015) satellite images were used for land cover classification by using ERDAS Imagine 2011 to detect land cover changes in the watershed. In order to assess the impact of land cover change on the stream flow HBV-96 semi-distributed hydrological model was used. The result of Landsat image analysis for the land cover of the watershed indicated that the forest lands cover decreased by 20% during 1973-1986 and by 37% during 1986-2015. There was great expansion of agriculture land by 7 %(1973-1986), and 60 %(1986-2015) respectively in the same period. The HBV-96 model results indicated reasonable model performance for periods of calibration (NS=0.7) and validation (NS=0.66). During total recording period from (1987-1995) stream flow volume was decreased by 27%. The peak flow increased by $0.34\text{m}^3/\text{s}$ and the base flow in the dry season also decreased by insignificant changes during the first period. For the record period the peak flow increased by 31% while base flow decreased by 38% for period of 1986-2015 during the land cover change. Generally, the analysis indicated that flow during the wet season has increased, while the flow during the dry season decreased. On account of land cover change in the watershed environmental flow is decreasing trend. This would likely have a direct effect on the Angreb (source of drinking water supply for Gonder town) and planned Megech dam (for irrigation) in the future. Therefore, there is a need to develop a new water management scenario to balance the stream flow due to the land cover changes. Effective Biological soil and water conservation practices with community participatory approaches would likely be used as one of remedial action for rehabilitation of the degrading environment from the land cover change in the watershed.

ACKNOWLEDGMENT

First of all I would like to thank the almighty GOD for giving me the audacity and wisdom to reach this point in life.

I would like to express my sincere gratitude to my supervisor, Mamaru A. Moges (PhD candidate) for giving me valuable guidance and support throughout my research. I am also indebted to my co-supervisor, Tesfaye Ababu, who contributes for the success of the thesis work and again thank you for his friendly advises.

Thanks to GOD, I have lots of exciting friends whom I met in my walk of life. Letters and words limit me to list your names. You all were great. I learnt a lot from you. Those of you I met during the study period thank you for those beautiful days we spent together.

At last but not least, I would like to extend my deepest gratitude to my beloved wife Letebrehan Abreha and my son Nuhamine Zemenu for sacrifices throughout the study period. Without your encouragement, tolerance and care this would not have happened.

I gratefully acknowledge the Ethiopian Ministry of Water Irrigation and Electricity, Amhara Region National Meteorological Services Bahir Dar branch and people who have given me data for my study, supporting and assistance they gave me during field work

TABLE OF CONTENTS

DECLARATION.....	- 962 -
Abstract.....	- 964 -
ACKNOWLEDGMENT	- 965 -
ACRONYM.....	- 972 -
Chapter One	973
1. INTRODUCTION.....	973
1.1 Introduction.....	973
1.2 Problem Statement.....	974
1.3 Objective (s) of the Study	974
1.3.1General Objective.....	974
1.3.2The Specific objectives:.....	974
1.4 Research Hypothesis.....	975
1.5 Significance of the Study.....	975
1.6 Research Questions.....	975
1.7 Thesis Outline.....	975
Chapter Two	976
2. LITERATURE REVIEW	976
2.1 Land Cover Classification.....	976
2.2 Land Cover Change Detection.....	976
2.3 Remote Sense and GIS for land cover classification.....	978
2.3 Hydrological Modeling.....	978
2.3.1Major Classification of Hydrological modeling	979
2.3.2HBV-96 model.....	979
2.3.4 Previous works in the study Area	980
Chapter Three.....	982
3. Materials and Methods	982
3.1 Description of the Study Area.....	982
3.1.1 Location	982

3.1.2 Topography	983
3.1.3 Climate	984
3.1.4 Land Cover	984
3.2 Methodology	985
3.2.1 Data availability and analysis	985
3.2.2 Hydro-meteorological Data Screening	986
3.2.3 Filling the missed data	988
3.2.4 Test for Consistency of the record	989
3.3 Material used	989
3.4 Image Processing	990
3.4.1 Geometric calibration	990
3.4.2 Radiance Calculation	991
3.5 Land Cover Image Classification	994
3.6 Change detection	995
3.7 Accuracy Assessment	996
3.8 HBV-96 Model	997
3.8.1 HBV-96 Model structure	998
3.8.2 Soil Routine	999
3.8.3 Response routine	1000
3.8.4 Model input	1001
3.9 Sensitivity, Calibration and Validation HBV-96 Model	1005
Chapter Four	1007
4. RESULT AND DISCUSSION	1007
4.1 Land cover classification	1007
4.1.1 Accuracy assessment	1007
4.2 Land cover classes	1008
4.2.1 Land cover class of 1973	1008
4.2.2 Land cover class of 1986	1009
4.2.3 Land cover class for 2007	1011
4.2.4 Land cover class of 2015	1012
4.3 Trends in land cover classes (1973-2015)	1012
4.4 Land Cover Trend Analysis for Last 10 years	1015
4.4 Hydrological Modeling Sensitivity Analysis, calibration and validation	1016
4.4.1 Sensitivity analysis	1016
4.4.2 Calibration	1019
4.4.3 Land Cover change Induce parameter changes	1023

4.4.4 Validation	1024
4.4.5 The effect of Angereb dam on Megech river flow.....	1027
4.4.5.1 Before Angereb dam construction (1973-1985)	1027
4.4.5.2 after dam construction (1986-2001)	1027
4.4.6 Effect of rainfall on Megech watershed.....	1028
4.4.7 Land cover change effect on Low flow.....	1030
<i>Figure 4.36 Observed and simulated low flows by using different period land cover maps baseline, 1986 and 2015.....</i>	<i>1031</i>
4.4.8 Flow Duration curve.....	1031
CHAPTER FIVE	1033
5. CONCLUSION AND RECOMMENDATION	1033
5.1 Conclusion.....	1033
5.2 Recommendation	1034
REFERENCES.....	1034
<i>Appendix A: Meteorological Stations, percentage missing and double mass.....</i>	<i>1039</i>
<i>Appendix B: Sensitivity Analysis of HBV model Parameters and Optimum Parameter Space.....</i>	<i>1041</i>
<i>Appendix C low flow</i>	<i>1041</i>
<i>Appendix D: Locations of Ground Control points in the Study Area</i>	<i>1042</i>

LIST OF TABLES

Table 3.2 Information On The Land Sat Image Acquisition Used For This Study	990
Table 3.6 Calculated Band Reflectance For Landsat 8.....	994
Table 3.7 Theissen Weight For Selected Stations In Megechwatershed Station.....	1001
Table 4.9 Base Error Matrix Of 2015 Land Cover Class	1007
Table 4.10 Accuracy Assessment Of 2015 Land Cover Class	1008
Table 4.11 Land Cover Class In Megech Watershed (1973, 1986, 2015).....	1013
Table 4.12 Summery Of Land Cover Changed In Different Time Periods In The Megech Watershed	1014
Table 4.13 Parameter Range Values For Hbv-96 Model.....	1016
Table 4.15 Land Cover Induce Change For 1986 And 2015.....	1023
Table 4.16 Summery Of The Result Of Calibration And Validation	1027
Table 4.17 Megech River Discharge Before And After Dam Construction.....	1027
Table 4.18 Angereb Dam Data (Source: Unesco, 2008)	1028
Table 4.19 Trend Of Annual Rainfall (1973-2001)	1029
Table A.1 Meteorological Stations And Percentage Missing (%).....	1039
Table B.1: Sensitivity Parameter	1041
Table C1 :1 Low Flow Data.....	1041
Table C3: Annual Maximum Stream Flow Table	C4: Total Stream
Flow	1042
Table D1 Gcp.....	1043

List of Figures

Figure 3.1 Location Of Megech Watershed.....	983
Figure 3.2 Elevation Map Of Megech Watershed (Elevation Units In Meter).....	984
Figure 3.3 -Land Covers Map Of Megech Watershed.....	985
Figure 3.4 -Meteorological Stations Selected In Megech Watershed For This Study.....	987
Figure 3.5-Rainfall (Mm) Data From The Shembekit Station (1986-1995).....	988
Figure 3.6 -Discharge Record Of Megech River At Azezo Station (1986-1995)	989
Figure 3.7 General Methodology Flow Charts For Land Cover Change Used In This Study ...	997
Figure 3.8 Schematic Structure Of Hbv-96 Model (Smhi, 2006).....	999
Figure 4.9 Theissen Polygon For Megech Watershed	1002
Figure 4.10 Land Cover Class And Relative Coverage From 1973 Landsat Image For Megech Watershed	1009
Figure 4.11 Land Cover Map Used As Baseline And Obtained From Mowie For Megechwatershed	1009
Figure.4.12 Land Cover Class And Relative Coverage From 1986 Landsat Image For Megech Watershed	1010
Figure 4.13- Land Cover Class And Relative Coverage From 1986 Landsat 5 Image For Megech Watershed	1010
Figure 4.17 Showed Agriculture Land Cover Was Found In Most Parts Of The Watersh	1011
Figure 4.18- Land Cover Class And Relative Coverage From 2007 Landsat 5 Image For Megech Watershed	1012
Figure 4.21 Land Cover Class Trend Analysis From 1973 To 2015.....	1013
Figure 4-22: Gully Erosion In One Of Many Locations Of Megech Catchment (Picture Taken By Zemenu A. 2015).....	1016
Figure 4.23 Sensitivity Analyses For Hbv_ Model Parameters Evaluated In The Relative Change Of Evaluation Criteria's In Megech Watershed	1018
Figure 4.24 Simulated And Observed Stream Flow Using Baseline Land Cover For Megech Watershed During Calibration Period.	1020
Figure 4.25 Scatter Plot Using Baseline (2008)Land Cover Of Megech Watershed For Calibration Period.....	1020

Figure 4.26- Simulated And Observed Stream Flow Using 1986 Land Cover Of Megech Watershed For Calibration Period	1021
Figure 4.28- Simulated And Observed Stream Flow Using 2015 Land Cover Of Megech Watershed For Calibration Period	1022
Figure 4.30 Simulated And Observed Stream Flow Using Baseline Land Cover Of Megech Watershed For Validation Period	1025
Figure 4.31 Scatter Plot Using Baseline Land Cover Of Megech Watershed For Validation Period	1025
Figure 4.32 -Simulated And Observed Stream Flow Using 2015 Land Cover Of Megech Watershed For Validation Period.	1025
Figure 4.34-Simulated And Observed Stream Flow Using 1986 Land Cover Of Megech Watershed For Validation Period.	1026
Figure 4.32-Scatter Plot Using 1986 Land Cover Of Megech Watershed For Validation Period	1026
Figure 4.35 Relation Of Rainfall And Runoff	1029
Figure 4.37 Flow Duration Curves Of Observed Low Flow And Using Baseline, 1986 And 2015 Land Cover In Megech Watershed.....	1032

ACRONYM

ANRS	Amhara National Regional State
DEM	Digital Elevation Model
DMC	Double Mass Curve
DN	Digital Number
ERDAS	Earth Resource Data Analysis System
GIS	Geographical Information System
GPS	Geographical Positioning System
HBV	Hydrologiska Byrans Vattenbalansavdelning
LC	Land Cover
NMSA	National Meteorological Service Agency
NS	Nash Sutcliffe Efficiency
SMHI	Swedish Meteorological and Hydrological Institute
SRTM	Shuttle Radar Topographic Mission
TM	Thematic Mapper
UTM	Universal Transfer Mercator
FDC	Flow Duration Curve
LF	Low Flow
MoWIE	Ministry of Water Irrigation and Electricity
RVE	Relative Volume Error
SWAT	Soil and Water Assessment Tool
LMIN	Radiance minimum band
LMAX	Radiance Maximum Band
QCALMIN	Quantize cal_min band
QCALMAX	Quantize cal_max band
AVHRR	Advanced Very High Resolution Radiometer

Chapter One

1. INTRODUCTION

1.1 Introduction

Land cover dynamics is driven by human actions also produces changes that would affect human life (Agarwal et al., 2002). In Ethiopia 84% and population live in rural areas and directly depend on Agriculture for its livelihood. Nationally the population increased with continued human encroachment in to natural resources and the community looking for water resource for various development activities in agricultural watersheds. Generally, the demands for land increases as population increases.

The impact of land cover changes is currently affecting developing counties especially agriculture based economies and rapidly increasing human populations. As many countries are currently experiencing rapid land cover change, concurrent with increased demands on public water supply, and ground water level is critical to issues of water resource management (Hornbeck et al., 1993). Series Land cover changes are caused by a number of natural and human driving forces (Konrad, 2005). From the human factors, population growth is the most critical in Ethiopia (Hurni, 1993). Land cover changes may have immediate and long-lasting impacts on terrestrial hydrology which have been described by Calder (1993). It alters the long term balance between rainfall and evapotranspiration and the resultant runoff. In the short term, land cover change may affect the hydrological cycle either through increasing or decreasing the water yield even eliminating the low flow in some circumstances (Croke et al., 2004). Savernake (1995) suggested that in the long-term the reductions in evapotranspiration and water recycling arising from land cover changes may initiate a feedback mechanism that results in reduced rainfall.

Research on stream flow patterns with respect to land cover dynamics enables assessment of sustainability of land cover change systems; because stream flows reflect on the hydrological state of the entire watershed. As stated by Calder (2002), the hydrological impact of land cover changes is a referencing issue and much research is necessary. The information can also be applied to forecast the likely effects of any potential changes in land cover on water resource systems. Generally, it is appropriate to use satellite remote sensing and Geographic information system (GIS) integrated with the hydrological modeling to analyses the hydrological response due to the land cover change. Therefore, this study was aimed to evaluate the response of stream flow due to land cover change. The study is important because similar studies have not been done before to this watershed and using HBV-96 model

as a stream flow evaluation tool. In addition, it is also important to study the watershed since it is as the growth corridor of the government of Ethiopia.

1.2 Problem Statement

Effect of dense populated areas reflect computation on the natural resource resulting deforestation, encroachment of communal grazing land and expansion of the residential area to rural and urban areas. This also aggravates soil erosion including gully erosion resulted from land cover change of the Watershed. In addition, this dynamic change of land cover is expected to affect the water balance of the catchment by changing the peak flow, ground water table, runoff and infiltration. In order to understand the dynamics of land cover impact on the water resources; Land cover detection for long time periods by using physical based distributed hydrological modeling is very vital. This could help in understanding the impact of land cover change on the stream flow of the watershed. Even though it is clearly known that there is a significant land use land cover dynamics, comparatively little is known about the influences of this land cover change and climate change on the stream flow of the study area. Thus, this gap has been identified as a considerable research thematic area to conduct how much those changes have been affecting the stream flow on this particular watershed. Therefore, in this study land cover change was analyzed for the past 42 years and the response of the corresponding hydrological variable (stream flow) will be also assessed.

1.3 Objective (s) of the Study

1.3.1 General Objective

The main focus of this study is to evaluate the response of stream flow as a result of long term land cover change in Megech watershed, Upper Blue Nile basin, Ethiopia.

1.3.2 The Specific objectives:

- To carry out the land cover classification from Landsat 1(1973), Landsat 5(1986) and Landsat 8(2015) images for Megech watershed.
- To detect the trends in land cover change from Landsat images in three time periods in Megech watershed.
- Calibrating and validating HBV-96 model in Megech watershed.

- Evaluating the impact of land cover change on stream flow.

1.4 Research Hypothesis

Land cover change in the watershed by large will be changed to agriculture and would likely affect the stream flow especially the environmental flows in the watershed.

1.5 Significance of the Study

The land cover change has a direct and indirect effect on the hydrological characteristics of a given watershed. Knowing the land cover trend helps to imply about the feature scenarios will happen and this also helps to give direction for decision makers for managing the watershed. Knowing watershed stream flow response through hydrological modeling's helps to gain an understanding of the hydrological system in order to provide reliable information for managing water resources in a sustained manner. It will also help to develop available information for researchers, technology institution and the local government for the purpose of integrated water resource management activities.

1.6 Research Questions

To address the research objective for this study the following questions should be answered:

1. What is the extent of the land cover change in the watershed?
2. Which types of land cover dominantly changed in the watershed?
3. How does the land cover change affect the stream flow in the watershed?

1.7 Thesis Outline

This thesis is organized by five chapters. The first chapter contains general back ground of the study. Under this chapter problem, research questioner and objective is presented. Second chapter explain relevant literature review on land cover classification using, remote sensing and GIS, hydrological modeling. The third chapter explains about methodology and material used for the study. The Fourth chapter presents the result and discussion from this study. Chapter five contains conclusion and recommendation of the study.

Chapter Two

2. LITERATURE REVIEW

2.1 Land Cover Classification

Land cover classification that is based on different spectral characteristics of the different material on earth surface (Kerle, 2004).which can use as land image that result need to be validate to assess its accuracy. General image classification serve specific objective is covert image data to thematic data context of application interest in thematic characteristics area (pixel) rather than its reflection value. Thematic characteristics such as land cover etc.

The digital image processing is the potential to automate land cover mapping. To realize this potential, image analysts have developed a family of image classification techniques that automatically sort pixels with similar multispectral reflectance values into clusters that, ideally, correspond to functional land cover categories. Two general types of image classification techniques have been developed: supervised and unsupervised techniques. In supervised classification, the analyst's role is to specify in advance the multispectral reflectance and admittance values typical of each land cover class.

Case of unsupervised classification does not define training fields for each land cover class in advance. That to be determines the correspondences between the spectral classes that the algorithm defines and the functional land use and land cover categories established by agencies like the U.S. Geological Survey (Cowen and Jensen, 1998). The example that follows outlines how unsupervised classification contributes to the creation of a high-resolution national land cover data set. After classification process of the thematic map is evaluated this map by accuracy using done with comparing some random choosing pixel of the image.

2.2 Land Cover Change Detection

The term land cover refers to the kinds of vegetation that blanket the Earth's surface, or the kinds of materials that form the surface where vegetation is absent. Land use, by contrast, refers to the functional roles that the land plays in human economic activities (Campbell, 1983).

An increasing population and growing demands more land was put under cultivation. Subsequently forest areas were cleared, encroaching agriculture into steep slopes and areas that were not

suitable for agricultural activities. The impact of Land cover change has become a central component on ground water recharge, base flow, infiltration and runoff assessment for managing Water resources at the main point of this thesis work.

Change detection is the process of identifying differences in the state of an object by observing it at different times (Singh, 1989). Change detection is an important process in monitoring and managing natural resources and urban development because it provides quantitative analysis of the spatial distribution of the population of interest area Macleod and Congation (1998) list four aspects of change detection which are important when monitoring natural resources including, i) Detecting the changes that have occurred, ii) Identifying the nature of the change, iii) Measuring the area extent of the change and iv) Assessing the spatial pattern of the change

The basis of using remote sensing data for change detection is that changes in land cover result in changes in radiance values which can be remotely sensed. Techniques to perform change detection with satellite imagery have become numerous as a result of increasing versatility in manipulating digital data and increasing computer power.

A wide variety of digital change detection techniques have been developed over the last two decades. Singh (1989) and Coppin and Bauer (1996) summarize eleven different change detection algorithms that were found to be documented in the literature by 1995.

The land cover change may result in environmental, social and economic impacts of greater damage than benefit to the area (Moshen A, 1999). Therefore data on land cover change are of great importance to planners in monitoring the consequences of land cover change on the area. Such data are of value to resources management and agencies that plan and assess land use patterns and in modeling and predicting future changes.

2.3 Remote Sense and GIS for land cover classification

Remote sensing is broadly defined as the art and science of obtaining information about an object without being in direct physical contact with the object (Colwell, 1983; Lillesand et al., 2004). The modern usage of the term 'Remote Sensing' has more to do with the technical ways of collecting airborne and space borne information. It was the launch of the first civilian remote sensing satellite in the late July 1972 that paved the way for the modern remote sensing applications in many fields including natural resources management (Tucker et al. 1983). The multispectral data provided by the on-board sensors led to an improved understanding of crops, forests, soils, urban growth, land degradation and many other earth features and processes

GIS is important to use the benefit of collateral information, such as digital elevation models, hydrology and soil maps (Jensen, 2005), which can be provided with the extracted information from remotely sensed images into GIS platforms. Thus, the integration of remotely sensed data with GIS data has the potential to improve the accuracy of results. The main advantage of GIS is that changes can be detected more clearly than with other techniques using multi-source data

In recent years, remote sensing and GIS have been commonly integrated for analyzing and mapping land use and land cover changes (Thapa and Murayama, 2009). Driving land use and land cover change maps into GIS applications has been done using supervised classification algorithms through remotely sensed software (Tripathi and Kumar, 2012).

Gahegan and Flack (1999) stated that the relationship between remote sensing and GIS partitioning has traditionally been that of supplier (remote sensing) and consumer (GIS). Remote sensing analysts have become avid consumers of GIS data as a means to add value to remotely sensed data and analysis (Franklin, 2003).

2.3 Hydrological Modeling

Hydrological modeling helps to understand the hydrological cycle and process in the watershed (Ragan, 1968; Betson and Marius, 1969; Rawitz et al., 1970). A model is representative of the real world in to conceptual world. The model flow processes that occur in the real world will simplify and it should be able to capture the dominant process at different time and space in the watershed. Many hydrologic phenomena are extremely complex and may never be fully understood. In engineering practices, hydrologic processes must firstly be understood and modelers must be able to simulate these processes

at desired spatial and temporal scales that match with the specific problem statement (Rientjes et al, 2007).

2.3.1 Major Classification of Hydrological modeling

The hydrological model is large range developed and classified at different ways. They are predictive or investigation. Major classified of hydrological model is given in the report of world meteorological organization (WMO, 1990) the model divided in two classes: deterministic model (models, which value of all parameters are uniquely defined and stochastic models (models having probability distributions in parameter space). In this study semi distributed HBV-96 model has used for simulating discharge by using time period land cover classes.

2.3.2 HBV-96 model

HBV model was originally developed at water balance section of the Swedish Meteorological and Hydrological Institute (SMHI) to predict water in flow of hydro power plant (Lindstrom et al., 1997). HBV-96 is model of the hydrological processes in a catchment used to simulate the runoff processes. It can be described as a semi-distributed conceptual model that allows dividing the catchment into sub basins and this sub-basins further divide into elevation and vegetation zones.

The model consists of subroutines for snow accumulation and melt, soil accounting procedure, routines for runoff generation and a simple routing procedure. It is possible to run the model separately for several sub-basins and then add the contributions from the entire sub-basin. Calibration as well as forecast can be made for each sub-basin for the basins of considerable elevation range a subdivision into elevation zones can be made. Each elevation zone can be further divided into different vegetation zones. Schematic structure of the model and its routines are presented.

Other model semi-distribution (grey-box) models are dividing the catchment into sub catchments. This sub catchment characterized is lumped. Parameters of semi-distributed models are partially allowed to vary in space by dividing the basin into a number of sub-basins. The model is simplified version of surface and/or sub-surface flow equation of physically-based hydrologic models (Beven, 2000). In Physically distributed models spatial resolution is accounted for by using probability distribution of input parameter across the basin.

Therefore, based on the objective these researches the model selected HBV-96 are continuous model determine flow during storm and inter-storm period. Model can applied at daily time step. Sensitivity

stream flow analysis General catchment response is characterized by measuring the discharge at outlet. This described by hydrograph is spatial and temporal response that determines variation of input such as rainfall. The sensitivity to model structure and parameter is critical for identifying few parameters which control the hydrological system (Kimand Delleur, 1997; Merritt et al., 2005; Sieber and Uhlenbrook, 2005). This issue of sensitivity was also tackled in the context of model calibration by Vrugtetal (2005), which proposed a combined parameter and state estimation framework to reduce the interaction between model/input errors and optimized parameter values.

2.3.4 Previous works in the study Area

Many Researchers studied on stream flow response the result of land cover land change with use of satellite image data and remote sensing and GIS application. Some of the woks done using HBV-96 include the following:

Kebede (2009) studied the effect of land cover change on stream flow of Gilgel Abay watershed with an area of 1656 Km². Landsat 7 images were used for land cover classification. The HBV-96 models were used to simulate stream flow under different land cover scenarios. The major finding the study indicated that forest cover decreased by 1.38% between the years 1973-1986, while it was 0.92% the year 1986-2011. Result from HBV-96 indicate that stream flow increased by 0.762 m³/s while Base flow decreased by 0.069m³/s.The overall result shows flow in the wet season increased, while flow in dry season decrease.

Rientjes et al. (2011) evaluated changes in land cover and rainfall in the upper Gilgel Abbay watershed indicated how changes affected stream flow in terms of annual flow, high flows and low flows. In the study land cover classes was based on Landsat image analysis. Results of the supervised land cover classification analysis indicated that 50.9% and 16.7% of the catchment area was covered by forest in 1973 and 2001, respectively. The study also concluded that the significant decrease in forest cover was mainly due to expansion of agricultural land.

These studies indicated that land cover change response on stream flow by using HBV-96 model. Land cover changes were analyzed only using two time period satellite images only. Therefore the uniqueness of this study was

1. The present study compares land cover from three time period satellite images i.e. Landsat 1 ,Landsat 5 and Landsat8

2. These study uses in the watershed where much similar studies has not been conducted.
3. This study mainly focuses on the watershed where future water resource development would be highly the target by the government e.g Gonder water supply reservoir (existing) and the Megech dam for irrigation (planned).

IJSER

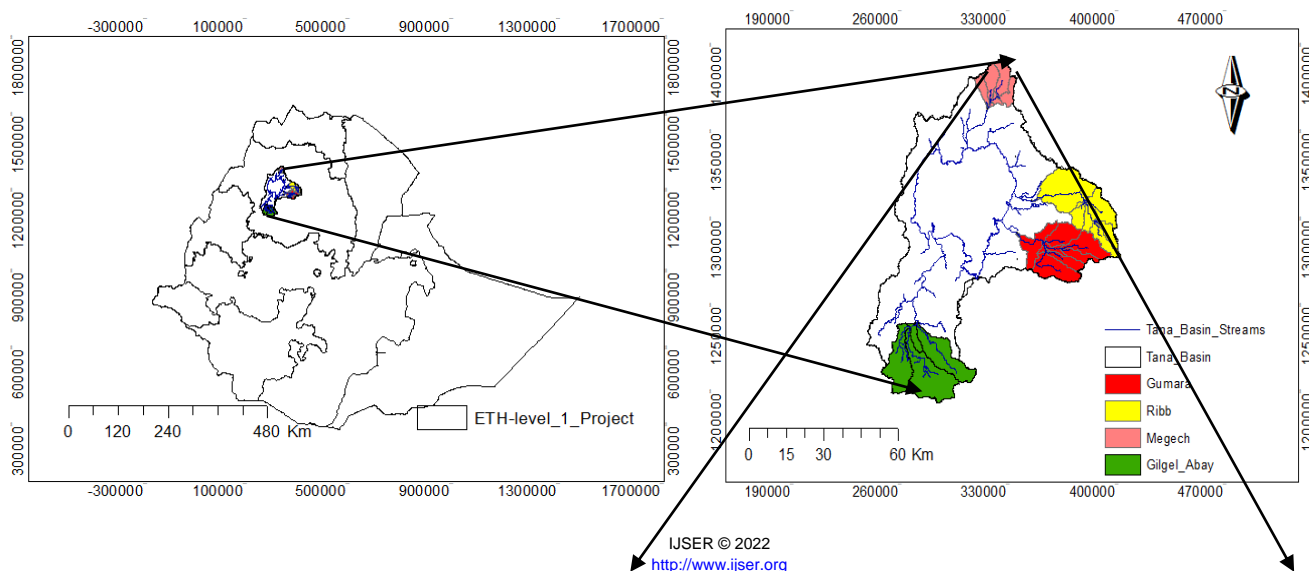
Chapter Three

3. Materials and Methods

3.1 Description of the Study Area

3.1.1 Location

The Megech River originates near the simian mountains National park where located in the Northwestern plateau of North Gondar zone Amhara National Region. The river is found in north-west Ethiopia which empties into Lake Tana at latitude $12^{\circ}d 29'$ longitude $37^{\circ} 27'$ E Coordinates: 331553 E longitude and 1380370 N latitude. Megech River measured at the Gauge station located at about the Azezo Gonder outlet of the watershed. The mean annual temperature ranges from $15^{\circ}c$ to $28^{\circ}c$. The basin receives about 1200mm rainfall annually, of which 25% about 85% falls during the wet season. Agriculture land is the dominant land cover in the basin of the total area. Soil in this river basin is predominantly sandy clay loam. More than 75 % of the total water withdrawal is used in the agricultural sector, mostly for irrigation. Owing to the traditional method of irrigation and water conveying systems .The maximum discharge $137m^3/s$ was obtained during the summer monsoon and the minimum discharge is $0.162m^3/s$ in peak dry season in the watershed.



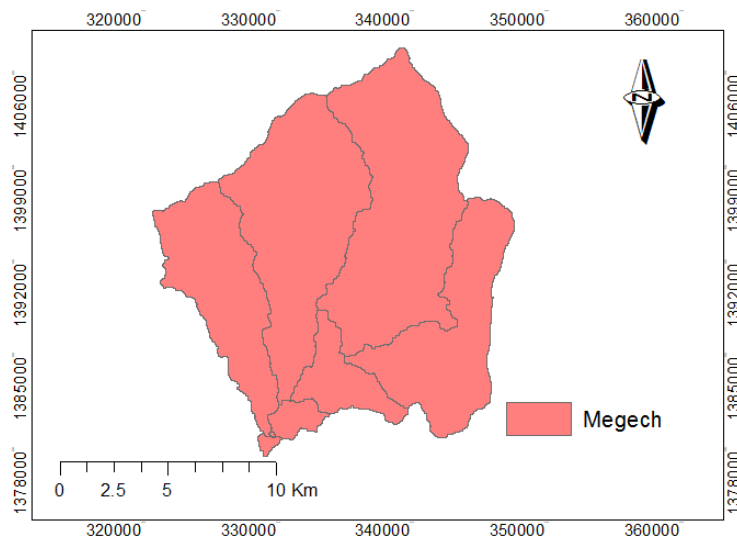


Figure 3.1 Location of Megech watersheds

3.1.2 Topography

The topography of the basin is mostly mountainous. The watershed range in altitude from around 1855 at outlet at basin to over 2950 m.a.s.l. The landscape of the area is highly rugged with high mountain ranges on the south and closely dispersed and their escarpments in the central and northern parts of the watershed, which are dissected deep and wide bedded gorges and valleys as well as plains on the top of the hills. The catchment topography and elevation level were estimated using a 30 m Digital Elevation Model (DEM). The elevation level of Megech sub-basin as detailed in below figure 3.2

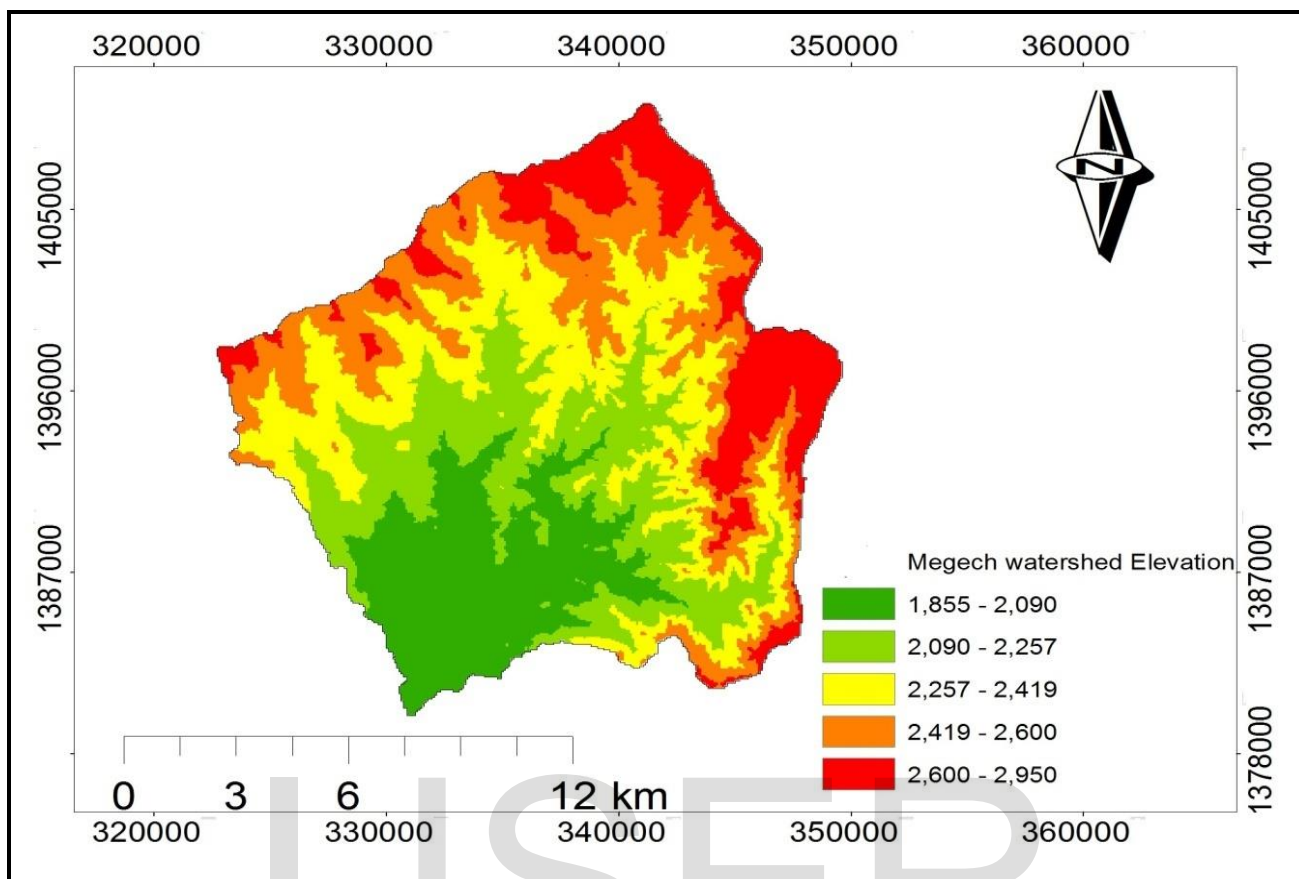


Figure 3.2 Elevation map of Megech watershed (elevation units in meter)

3.1.3 Climate

The climate in the study area is characterized by two distinct seasons: a wet season (June to August) and a dry season (January to March). The mean annual temperature ranges from 25 to 28°C. The basin receives about 1200mm rainfall annually, of which about 85% falls during the wet season. Woods and shrub land are the dominant land cover in the basin of the total area

3.1.4 Land Cover

Megech watershed land cover map was obtained from MoIWE and was divided into three and reclassified for input requirement. Based on MoWIE (2008) the major dominant land cover types of the Megech was mainly covered by cultivated land (98.27%), Grass and shrub coverage (0.5 %) and urban was 1.22%.

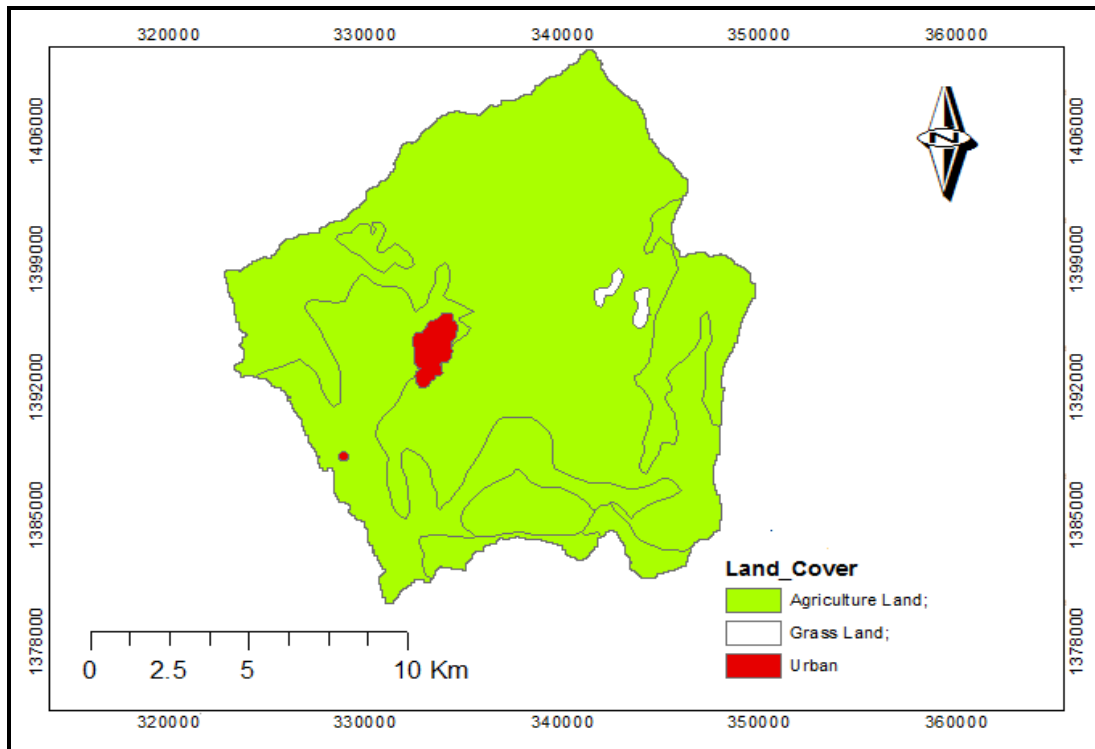


Figure 3.3 -Land covers Map of Megech watershed

3.2 Methodology

3.2.1 Data availability and analysis

The data necessary for this study were obtained from national institution and international websites. The meteorological data was obtained from National Meteorological Agency, Bahir Dar branch (Table 1). The stream flow data was obtained from the Ministry of Water Irrigation and Electricity (MoWIE). Filling the missed values of the collected data of the stations, maintaining quality of the data/ detecting outliers for precipitation and temperature were carried out.

Table 3.1 Data availability of station information

Station Name	Period	Maximum	minimum	Average	Location	Station Weight (%)
Shambiket(RF)	1986-1995	110(mm)	0(mm)	2.47(mm)	Inside watershed	82
Gonder(Temperature)	1986-1995	29(°c)	0 (°c)	15(°c)	Outside Watershed	18

Average monthly potential evapotranspiration in mm/day from 1986-1995 was available for Gonder stations only. The values of PET were calculated by simple temperature method (Enku and Melesse, 2014).

3.2.2 Hydro-meteorological Data Screening

A time series of hydrological data for hydrological model should have to existing primary data screening such as sationarity, inconsistency. The basic data-screening procedure used here is based upon split-record tests for stability of the variance (F-test) and stability of mean (t-test) of such a time series. A time series of hydrological data may exhibit jumps and trends owing to what Yevjevich and Jeng (1969) call inconsistency and non-homogeneity. Inconsistency is a change in the amount of systematic error associated with the recording of data. It can arise from the use of different instruments and methods of observation. Non-homogeneity is a change in the statistical properties of the time series. It can because either natural or man-made. These include alterations to land use, relocation of the observation station, and implementation of flow diversion. The data screening procedure passed through the following principal steps in order to check the absolute and relative consistency, homogeneity and sationarity of the data, for the selected stations.

1. Rough screening of the data and compute or verify the totals for the hydrological year or season.
2. Plot these totals according to the chosen time step (yearly for this study) and note any trends or discontinuities (visual examination).
3. Test the time series for absence of trend with Spearman’s rank-correlation method.
4. Apply the F-test for stability of variance and the t-test for stability of mean to the split, non-overlapping, sub-sets of the time series at the 5-percent level of significance;
5. Test the time series for absence of persistence by computing the first serial-correlation Coefficient (used only for flow data);

6. Test the time series for relative consistency and homogeneity with double-mass analysis. Two metrological stations for the study area which are absolutely consistence and Homogenous are selected.

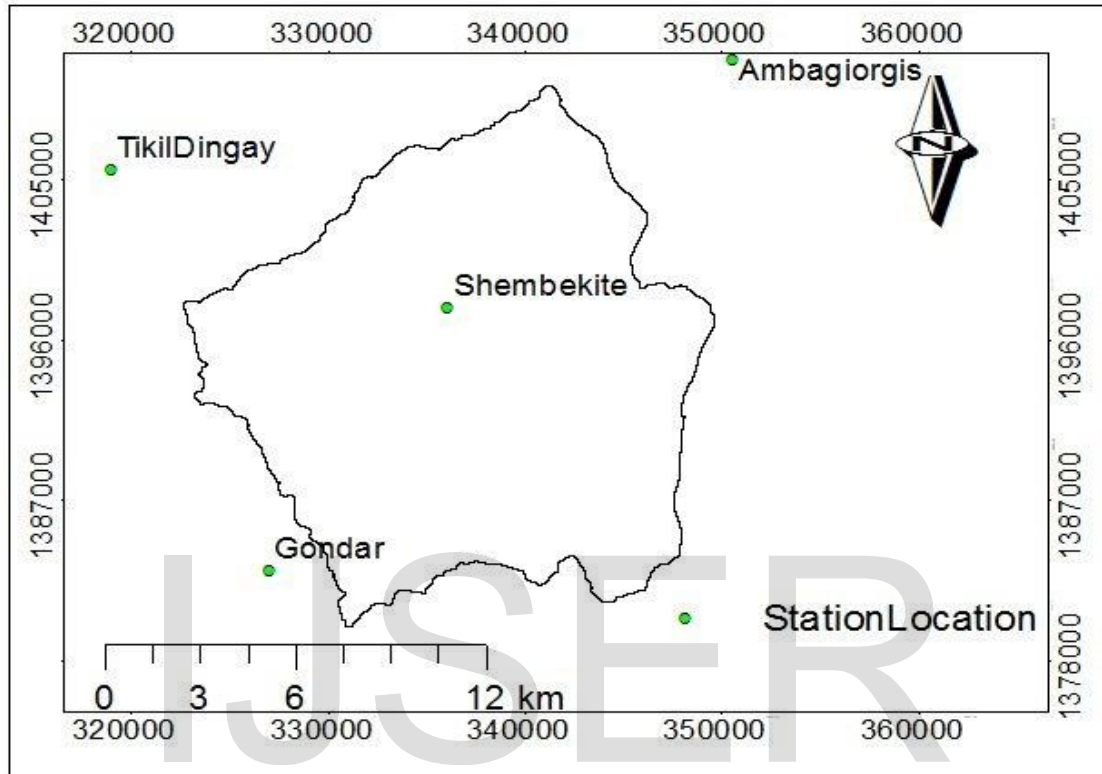


Figure 3.4 -Meteorological stations selected in Megech watershed for this study

On the other hand use of low flow analysis calculated for this study was based on the seven day sustained low flow (7D slf).This was carried out by taking one last value from the last 7 similar values or considering the average of the lowest 7 records of stream flow from each year.

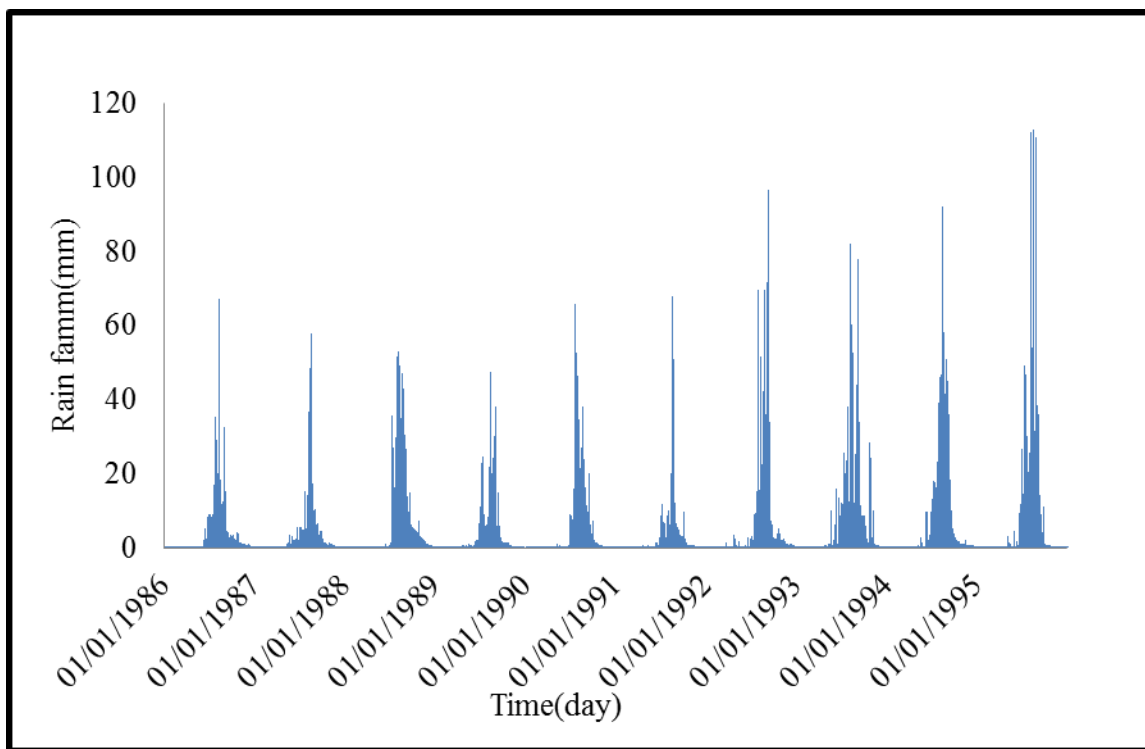


Figure 3.5-Rainfall (mm) data from the Shembekit station (1986-1995)

3.2.3 Filling the missed data

Filling the missed data can be done in different ways one of the methods is choosing based on the data percentage of the missing as recommended by Chow (1964) .Stations with percentage error less than 10% missing data can be filled by normal ratio method. Missing data percentage greater than 10 should be filled by linear and non- linear regression method. For this specific study Shembekit station percentage has missing data proportion of 9.27% and Gonder 7%.Hence for both stations the normal ratio method (Eqn 3.1) were used to fill the missed data.

$$P_X = \frac{N_X}{n} \left(\frac{P_1}{N} + \frac{P_2}{N_2} + \dots + \frac{P_n}{N_n} \right) \tag{3.1}$$

Where: P_X =Missed value of precipitation to be computed, N_X = average value of rainfall for the station in question for recording period, N_1 = average value of rainfall for the neighboring station, $P_1, P_2 \dots P_n$ = rainfall of neighboring station during missing period and n = number of stations used in the computation

Data of Megech river flow was collected from the MoWIE from 1986-1995near Azezo gage station. The annual minimum discharge ranges from $0.004\text{m}^3/\text{s}$ while the maximum discharge $110.8\text{m}^3/\text{s}$ (Figure 3.6).

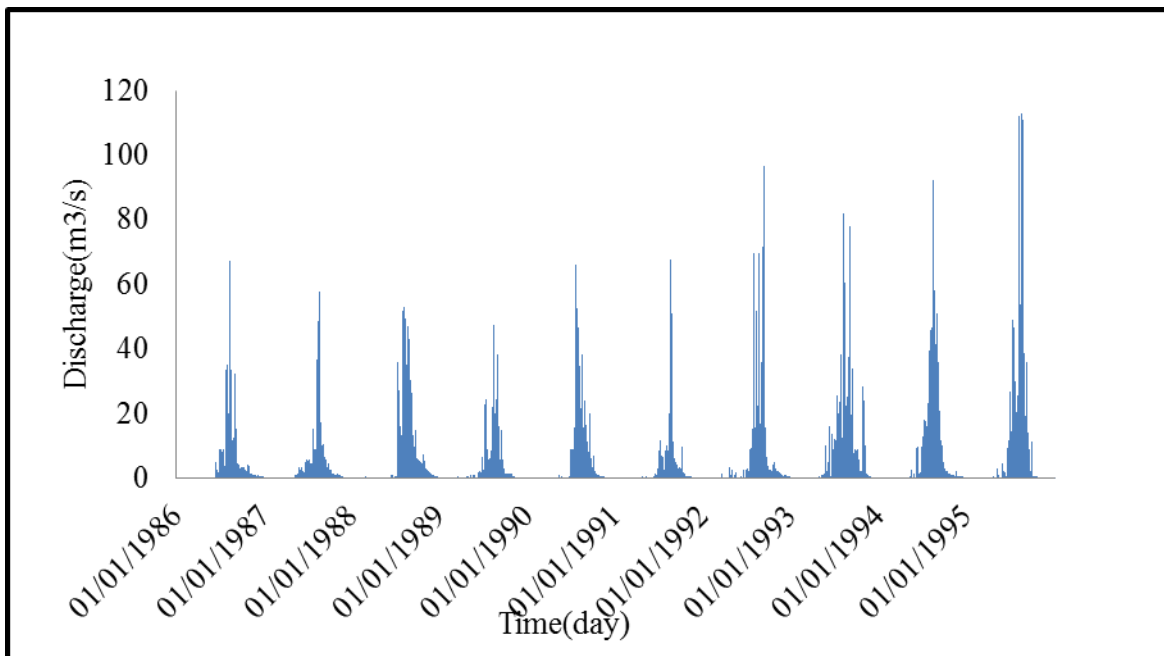


Figure 3.6 -Discharge record of Megech River at Azezo station (1986-1995)

3.2.4 Test for Consistency of the record

Rainfall data analysis from the station may not be consistent always. Many factors could affect the consistency of the record at studies station .To check and correct the consistency of a record Double Mass Curve (DMC) have been used .This method uses the accumulated annual rainfall of studies site station versus the cumulative rainfall of all station surrounding base stations. If rainfall record in a given station is consistent then the double mass curve will have a constant slope otherwise there is inconsistency in the measured value. Based on double mass curve result all station was found consistent (Petra, 2001). The data and the analysis of DCM can be found at Annex (Table A2 and Figure A1)

3.3Material used

The materials used for this study includes Arc GIS 10.1 software used for delineating, discretization of watershed and land cover classification in Megech watershed. HBV-96 (Bringstorm, 1970) hydrological water balance model for analyzing land cover induced stream flow in the watershed. GPS used to collect the ground control point and altitude of locations in the sub basin. Earth Resource Data Analysis System (ERDAS IMAGE 11) software is which used to incorporate Land sat images to identify changes in land cover distribution in the study area. Already existing soil data are the materials used in this study

3.4. Image Processing

The three times series Land sat 1,5 and 8 image are used to identify land cover change distribution for Megech watershed for over 42 year’s period from 1973 -2015. In this study three images have been selected to present land cover change in the year 1973, 1986, and 2015 using Landsat MSS, TM and ETM+ respectively. The satellite image are acquired at dry month the reason to get better atmosphere condition (reduced cloud cover).There would be clear image for dense forest vegetation and pieces of agriculture plot and difference reflectance between grazing and agriculture plot. The selected Landsat image of the Megech catchment cloud cover show less than 10% for the acquisition date of the image (January 1973, 1986 and, 2015).

Land cover map were prepared through the three time series period image classification tool was used ERDAS IMAGINE 11. The download image file format is *.tiff coordination system is used UTM projection, WGS 1984 datum and zone 37 N that used in ERDAS IMAGINE. The Landsat images used for this study were loaded from www.earthexplorer.com including acquisition dates, sensor, path /Row, here summarized in the (table3.2) below.

Table 3.2 Information on the land sat image acquisition used for this study

S/No.	Sensor Instrument	Satellite Name	Path	Row	Date of acquisition	Spatial Resolution
1	Landsat TM	Landsat5	170	51	January03,1986	30
2	Landsat TM	Landsat8	170	51	January03,2015	30
3	Land sat TM	Land sat 1	182	51	January 03/1973	30

3.4.1 Geometric calibration

Remote sensing images are rarely provided in the correct projection, coordinate system and free of geometric distortions. Geometric distortions occur due to earth rotation during acquisition and due to earth curvature. In order to combine images with other digital map data they must be transformed from the acquisition coordinate system (rows/columns) to that of the digital map data sets. For well-defined orbital geometry parameters this can be achieved using predefined transformations (Mather, 1995 and, 1999).The adjustment transformation model includes the aspect, skew and rotational distortions of a

sensor. However, not all possible causes of geometric distortion can be modeled using these predefined transformations - therefore a more general approach is required e.g., using ground control data. The download images are in the form of grids where each grid is assigned with a certain digital number called Digital Number (DN) value.

Digital number is a value assigned to a pixel. It must be converted to actual reflectance values using the calibration constants specific to the sensor. The calibration constants are often provided with the image in a separate text file. The user shall read this file and collect all the required information to calibrate the image. Therefore in this study we used this file to calibrate the images for land cover classification in the watershed.

Table 3.3 Meta data information obtained in Landsat 5 in 1986.

Parameter	Satellite Bands						
	B1	B2	B3	B4	B5	B6	B7
L _{max}	169	333	264	221	30.2	15.303	16.5
L _{min}	-1.52	-2.84	-1.17	-1.51	-0.37	1.238	-0.15
QCAL _{max}	255	255	255	255	255	255	255
QCAL _{min}	1	1	1	1	1	1	1
Sun-Azimuth	127.83	127.83	127.83	127.83	127.83	127.83	127.83

Table 3.4 Meta data information obtained in Landsat 8 in 2015.

Parameter	Satellite Bands					
	B1	B2	B3	B4	B5	B7
L _{max}	783.3	802.11	739.14	623.28	381.41	31.97
L _{min}	-64.68	-66.23	-61.03	-51.47	-31.49	-2.64
QCAL _{max}	65535	65535	65535	65535	65535	65535
QCAL _{min}	1	1	1	1	1	1
Sun-Azimuth	144.3	144.3	144.3	144.3	144.3	144.3

3.4.2 Radiance Calculation

In order to calculate the radiance from DN value the following equation (3.2-3.4) we used To summaries the relationship between radiance (L) and pixel DN look at below to Formula. As pixel DN is a simple linear transformation of radiance, the slope and offset of this linear transformation

(which is specific for each spectral band, each sensor and initial calibration) can be used to calculate radiance (L) and inversely used to calculate pixel DN value. Radiance-to-DN and one for the DN-to-radiance

$$DN = \frac{DN_{max}}{L_{max} - L_{min}} (L - L_{min}) \text{ -----3.2}$$

$$L = \frac{L_{max} - L_{min}}{DN_{max}} * DN + L_{min} \text{ -----3.3}$$

That is L= gain *DN+offset which can be thought of as L=slope *DN+intercept

Measured in W·m⁻²·sr⁻¹· μ m⁻¹

L can also be estimated using another method as:

$$L_{\lambda} = \left(\frac{L_{max \lambda} - L_{min \lambda}}{QCAL_{max} - QCAL_{min}} \right) * (DN - QCAL_{min}) + L_{min \lambda} \text{ ---- 3.4}$$

Where L_λ is the radiance in Wm⁻²sr⁻¹μm⁻¹, L_{max λ} is the maximum radiance for a given wave length that can be measured by the sensor, L_{min λ} is the minimum radiance for a given wave length that can be measured by the sensor, QCAL_{max} is Maximum DN value possible, QCAL_{min} is Minimum DN value possible, DN is the digital number (pixel value).

3.4.3 Calculating reflectance

Reflectance is the ratio between reflected and incoming radiation. The reflected energy is the one measured by the satellite while the incoming is the one coming from solar radiation. The measured energy is estimated by using.

$$ESUN_{\lambda} COS \theta_z \text{ ----- 3.5}$$

While the incoming is the one coming from solar radiation was estimated by:

$$L_{\lambda} \pi d^2 \text{ --- --- 3.6}$$

Where L_{λ} is the radiance at sensor in $Wm^{-2}sr^{-1}\mu m^{-1}$, d is the earth – sun distance (Astronomical units), θ is the solar zenith angle (degree) and ESUN is band dependent exoatmospheric Irradiance ($Wm^{-2}\mu m^{-1}$).

$$d = 1 + 0.01672 * \sin\left(\frac{2 * \pi * (J - 93.5)}{365}\right) \text{ --- --- --- 3.7}$$

Where d is the earth – sun distance (Astronomical unit), J is in Julian days and \sin is in radians.

It should be noted reflectance does not have units and is measured on a scale from 0 to 1 or from 0-100% in percent.

3.4.4 Earth-Sun distance

Earth distance as the variable for calculating reflectance can be estimated using Eqn. 3.8

$$ESUN_{\lambda} = \frac{\sum(RSR * SolarIrradiance) * \Delta\lambda}{\sum(RSR) * \Delta\lambda} \text{ --- --- --- 3.8}$$

Where, RSR is the relative spectral response specific to the sensor and the band (shown below). Now fill the respective values in the table below after calculating using the formulae given above.

Table 3.5 Calculated bands reflectance for Land sat 5

Reflectance parameter	B1	B2	B3	B4	B5	B7
D^2	0.99	0.99	0.99	0.99	0.99	0.99
ESUN	1957	1826	1554	1036	215	80.67
$\text{Cos}\phi$	0.67	0.67	0.67	0.67	0.67	0.67

The reflectance for the respective band except band 6 was calculated by using

$$\rho_p = \frac{\pi * L_\lambda * d^2}{ESUN_\lambda * COS\theta_z} \text{-----} 3.9$$

The solar zenith is the 90 minus the sun elevation provided in the ancillary file. Adapt the statement you created for band one to calibrate all other bands.

Table 3.6 Calculated band reflectance for Landsat 8

Reflectance parameter	B2	B3	B4	B5	B6	B7	B9
	(Blue)	(Green)	(NIR)	(NIR)	(SWIR)	(SWIR)	(SWIR)
D ²	0.98	0.98	0.98	0.98	0.98	0.98	0.98
ESUN	2067	1893	1603	972.6	245	79.72	399.7
Cosφ	0.75	0.75	0.75	0.75	0.75	0.75	0.75

3.5 Land Cover Image Classification

For the purpose of classifying the land cover during image analysis the land cover types were defined (table 3.7). During the field cross observation five different types of land cover have been identified for the Megech catchment as described in table 3.7

Table 3.7 land cover class description for Megech watershed (based on field observation)

Type of land cover class	Description of land covers
Forest Land	High density of trees which include deciduous forest land, ever green forest land, mixed forest land and plantation forests that mainly are eucalyptus, junipers and conifers
Agriculture Land	Areas used for both annual and perennial crop cultivation, and the large sized cultivated fields.
Shrubs and Grass land	Areas covered with shrubs, bushes and small trees, with little wood, mixed with some grass .Area covered with grass that is used for grazing
water area	Area which remains open water area throughout the year, the man made water harvesting ponds, the rivers and its main tributaries
Built Up Area	This type of land cover of rural settlements area and Urban area, Transportation, Institution

Satellite image (Land sat, 1, 5 and 8) classification for land cover class depends on spectral classes that suited to particular classifier algorithm used (Kelly, 1984). In this study, land cover for the selected date was estimated using the supervised image classification (Campbell, 2002). For the supervised classification, the ground control points collected in the field were used as the training sample set. Supporting information was obtained from field observation of the land cover, interviews with local elder people and topographic maps. It is also achieved by calculating a statistical distance based on the mean values and covariance of the clusters. The spatial coverage of each land cover class can be visualized on three of historical land cover map. In general, a total of five major land cover classes were selected in after the observation during the field work five different types of land cover have been identified for this catchment: agricultural land, grass land, shrubs land, forest land, and water and marshy land.

For supervised classification method 200 Ground Control points were collected in the field as the training samples set on all land cover types (Annex D:Table 1GroundControlPoint).Supporting information collected during field observation of in watershed and interview with local farmers. Which were used for image classification of the pixels into similar groups based on sample signature specific. The prepared band and color combination of Landsat image of 7, 5 and, 3 for (2015); 7, 4, 2 for (1986) and 4, 2, 1 for (1973) interpretation of the image in their true color.

The classification was performed by assigning the pixels in the sample set using the maximum likelihood method (Campbell, 2002). It uses probability that a pixel belongs to a particular class and the basic equation assumes that those probabilities are equal for all class and that the input bands have normal distribution. It was selected due that its consideration of the spectral variation within each category and overlap that may occur among different classes.

3.6Change detection

Change detection is the process of identifying change that might have occurred in the interval between the two dates (Singh, 1989). There is a large number of change detection techniques developed and used over the years to estimate changes using remote sensing data. Change detection techniques includes image overlay, image digitizing, image differencing, image regression, image rationing, vegetation index differencing, principal component analysis, spectral and temporal classification, post classification comparison, change vector analysis, and background subtraction (Coppinand Bauer, 1996).There is no agreement as to a 'best' change detection approach. These methods have been successfully applied in monitoring changes detection. For this study, post classification comparison technique has been used to

determine the changes in land cover over 42 years (1973-2015). The advantage of post classification comparison was it simplifies the difficulties associated with the analysis of the images acquired at different times of the year, or by different sensors and quite high change detection accuracy (Alphan, 2003). This the most common approach to change detection and the methods comparison uses separate classifications of the images that occurred at different moment in time to produce different maps from which “from-to” change information can be generated (Jensen, 2004).

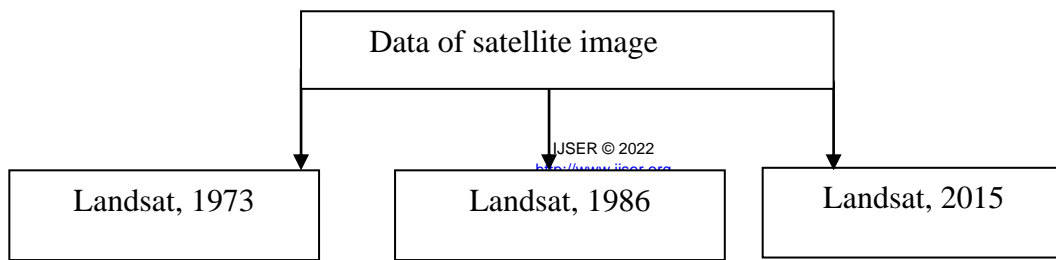
3.7 Accuracy Assessment

Accuracy assessment is part of the image classification process and its objective was to evaluate the total number of correctly classified pixels divided by the total number of ground truth pixels. User’s accuracy and producer accuracy measured the correctness of each category with respect to errors matrix. The users’ accuracy is defined as the probability that a reference pixel has been correctly classified as well as the producer accuracy is defined as the probability that a pixel classified on the map represents that class on the ground (Anderson, 1976).

The accuracy of thematic maps was determined by the constructed matrices along kappa statistics in order to test whether any difference exists in the interpretation. Kappa statistics (Eqn.3.10) considers a measure of overall accuracy of image classification and individual category accuracy as a means of actual agreement between classification and observation. Landis (1986) defined the agreement criteria for kappa statistic, the agreement is poor when $k < 0.40$, good when $0.4 < k < 0.7$ and excellent when $k > 0.75$. Alternatively, Monserud (1990) suggested the use of subjective kappa value as $< 40\%$ as poor, $40-55\%$ fair, $55-70\%$ good, $70-85\%$ very good and $> 85\%$ as excellent. The generally the estimate of Kappa was computed as follows

$$K = \frac{P_o - P_c}{1 - P_c} \text{ --- (3.10).}$$

Where, P_o = proportion of observed agreements, P_c = proportion of agreement expected by chance.



IJSER

Figure 3.7 General methodology flow charts for land cover change used in this study

3.8 HBV-96 Model

HBV-96 hydrological water balance model was originally developed by Swedish Meteorological and Hydrological Institute (SMHI) to predict the inflow of hydropower plants in the 1970s. It is a semi distributed model by dividing the basin into sub basins whereas a lumped model, it is assumed that the

study area (basin) is one single unit or zone and the parameters do not change spatially across the watershed. The model can also use for water balance studies to forecast runoff, to compute design flood for dam safety, to assess and simulate hydrologic responses due to the effect of land cover and climate change. HBV-96 uses general water balance model described under Eqn 3.11.

$$P - E - Q = \frac{d}{dx} [SP + SM + UZ + LZ + Lakes] \text{-----} 3.11$$

Where, P = precipitation, E = Evapotranspiration, Q = runoff, SP = snowpack, SM = soil moisture, UZ = upper groundwater zone, LZ = lower groundwater zone and Lakes = lake volume

3.8.1 HBV-96 Model structure

The HBV-96 is described as a semi-distributed conceptual model that allows dividing the catchment into sub basins and this sub basins further divide into elevation and vegetation zones. The model simulates daily discharge using daily rainfall, temperature and estimates of average monthly potential evapotranspiration as input. In addition sub basin spatial data derived from the mean catchment elevation and vegetation zones will be used as input.

The model consists of subroutines for snow accumulation and melt, soil accounting procedure, routines for runoff generation and a simple routing procedure. The model could be run separately for several subbasin and then add up from each sub basin to provide the response at the outlet of the watershed. Calibration in the HBV-96 model would be done by using the observed data at the outlet of the watershed. For this study calibration was done at the outlet of Megech watershed using the observed data collected from the gauging station near Azezo. The overall effect of elevation zone with respect to different vegetation zone (forest and field) was also considered by dividing the catchment in to the five sub basins. The zonations were done based on elevation and land cover data of each subbasin. During the whole period of study, the largest forest and field land cover zone were found at subbasin 4, and it is the highest elevated area next to subbasin 1. Land cover zones in each subbasin for three different periods are summarized as (table 3.8).

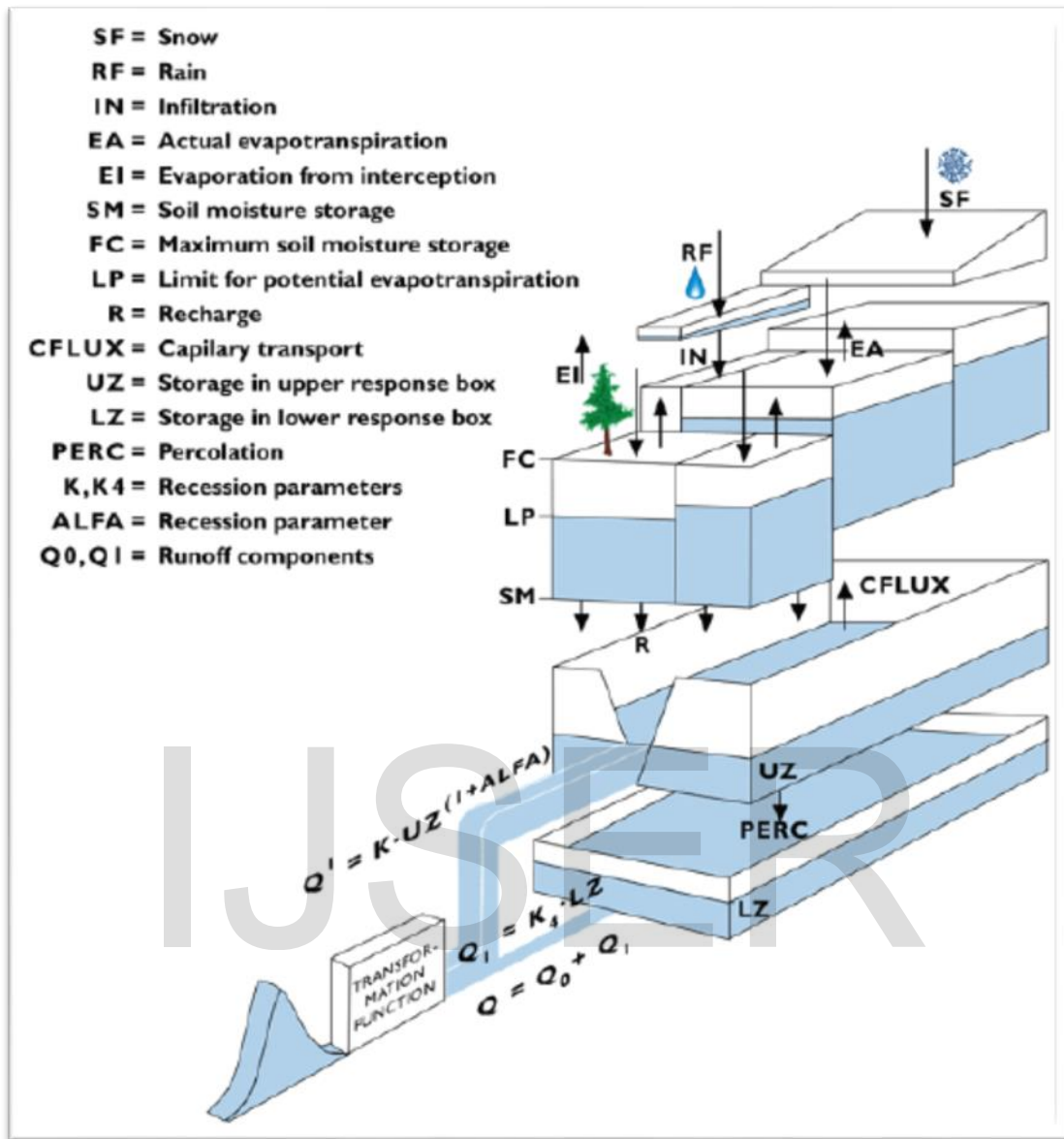


Figure 3.8 Schematic structure of HBV-96 model (SMHI, 2006)

The model consists of subroutines for precipitation and snow accumulation, for soil moisture accounting where ground water recharge and actual evaporation are coupled, and it consists of response routines, a transformation function and a simple routing procedure.

3.8.2 Soil Routine

Soil moisture routine is based on three parameter beta (β), limit for Potential Evapotranspiration (LP) and Field Capacity (FC). Beta controls the contribution to the response function and the increase in soil moisture storage, LP is the soil moisture value above which Evapotranspiration reaches its potential

value and FC is the maximum soil moisture storage in the model. The soil moisture is expressed as follows.

$$\frac{\Delta Q}{\Delta P} = \left(\frac{SM}{FC}\right)^\beta \text{ ----- 3.12}$$

(Seibert, 1997)The relation between the soil moisture and Evapotranspiration in HBV model can be expressed as:

$$E_a = E_p \left(\frac{SM}{LP * FC}, 1 \right) \text{ --- 3.13}$$

Where: SM is computed soil moisture storage, ΔP is contribution from rainfall, ΔQ is contribution to the response function, FC is maximum soil moisture storage, β is Empirical coefficient, E_p is potential Evapotranspiration, E_a is compute actual Evapotranspiration, and LP is limit for potential Evapotranspiration.

3.8.3 Response routine

The runoff response routine function is used to transform excess water from the soil moisture zone runoff. The routine consists of one upper reservoir and one lower reservoir. The storage in the upper reservoir will receive the yield from the soil moisture zone. If the yields from the soil moisture routine exceed its percolation capacity, the upper reservoir starts to fill. By then the water will percolate to the lower reservoir. The lower reservoir conceptually represents the ground water that contributes to the base flow of the watershed. In the model the outflow from the upper reservoir is estimated as follows

$$Q_o = k * UZ^{(1+\alpha)} \text{ ----- 3.14}$$

The outflow from the lower reservoir is described as follows:

$$Q_1 = K4 * LZ \text{ ----- 3.15}$$

Where Q_0 is direct runoff from upper reservoir, K is recession coefficient upper reservoir storage, Q_1 is lower reservoir outflow, LZ is lower reservoir storage, and K_4 is recession coefficient of lower reservoir storage.

The soil routine parameters FC , LP and β characterizes to influence the total flow volume, whereas the response parameters, k_4 , $perc$, khq , HQ and α influence the shape of the hydrograph. Since Hq is not calibrated, its value calculated as follows:

$$Hq = \frac{(MQ * MHQ)^{\frac{1}{2}} * 86.4}{A} \text{-----} 3.16$$

Where MQ is mean of the observed discharge flow over the whole period (m^3/s), MHQ is mean annual peak flow (m^3/s) and A is the area of the watershed (km^2)

3.8.4 Model input

3.8.4.1 Elevation Data

In HBV model the sub basin was classified based on mean elevation of 30m. Digital Elevation Model (DEM) was used to delineate the watershed and classify the mean elevation zones for the model input. In this study the 30 meter resolution DEM was used. The DEM was obtained from *USGS website* www.earthexplorer.com

3.8.4.2 Precipitation and Temperature data

HBV model requires an input such as daily precipitation and temperature data to perform the water balance of the watershed. For this study precipitation and temperature data from 1986-1995 was used from stations of Gonder and Shermbekit. In addition the weight for each precipitation stations was used as input. In order to the model determine for determining the areal rainfall of the watershed. The weight for each meteorological station was made by Thiessen method as indicated in the table 3.7 and figure 3.11

Table 3.7 Thiessen weight for selected stations in Megech watershed station

Station Name	Longitude (Decimal Degree)	Latitude (Decimal Degree)	Elevation (meter)	Area (Km ²)	Weight (percent)
Rainfall					
Shermbekit	37.49	12.64	2460	379.4	0.82
Gonder	37.42	12.55	2083	119.8	0.18
Total				499.2	1

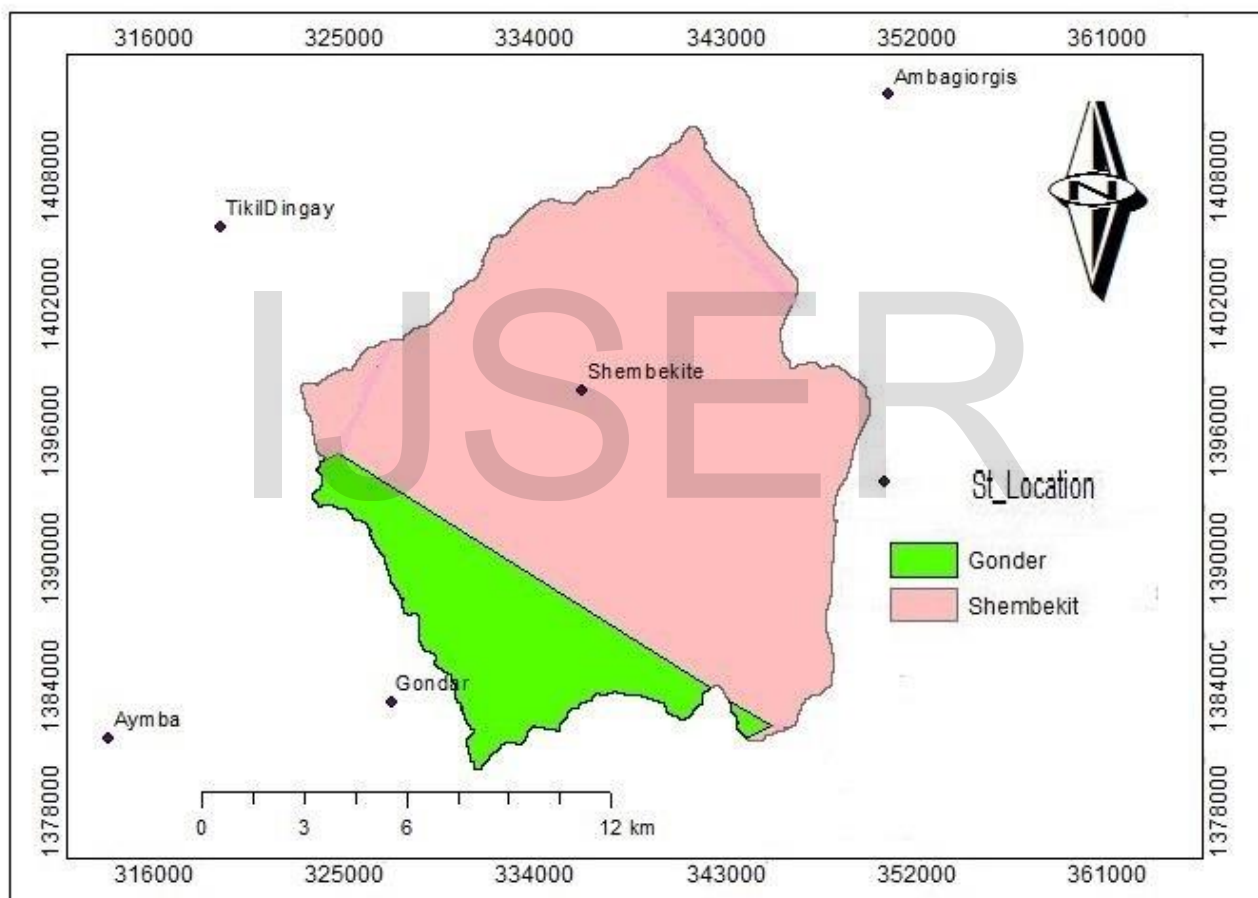


Figure 4.9 Thiessen Polygon for Megech watershed

3.8.4.3 Land Cover

The land cover as one important input for HBV-96 modeling input was classified in to three major land cover types which are: cultivated, forest, shrub and grass, and built up area. The model considers the

forested land cover as a unit and non-forested as one unit which is named as “field”. The average elevation class for user defined and selected sub-basins are summarized in table3.8

Table 3.8 Land cover zones and area coverage in each sub basin for 2015, 1986, 1973 and MOWIE prepared for HBV-96 model sub basin discretization.

Year	Name		Sub basin 1	Sub basin 2	Sub basin 3	Sub basin 4	Sub basin 5	Total area
2015		ME(m)	1990	2373	2770	2900	3335	
	LCZ	Field(km2)	238.58	92	93	34.86	0.33	458.77
		Forest(km2)	12.19	8	15	5	1	41.19
		Total (km2)	250.77	100	108	39.86	1.33	499.96
1986		ME(m)	1990	2373	2770	2900	3335	
	LCZ	Field (km2)	90	40	25	17.55	5	177.55
		Forest (km2)	3	40	60	70.3	150	323.3
		Total (km2)	93	80	85	87.85	155	500.85
MoWIE,2008		ME(m)	1990	2373	2770	2900	3335	
	LCZ	Field (km2)	270	160	40	20	7.4	497.4
		Forest (km2)	1	0.6	0.4	0.23	0.3	2.53
		Total area	271	160.6	40.4	20.23	7.7	499.93
1973		ME(m)	1990	2373	2770	2900	3335	
	LCZ	Field (km2)	65.44	15	10	12	5	107.44
		Forest (km2)	90.5	102	98	50	52	392.5
		Total area	155.94	117	108	62	57	499.94

3.8.4.4 Evapotranspiration

The HBV model requires monthly long-term mean potential Evapotranspiration (SMHI, 2006) data. There are a lot of methods to estimate Evapotranspiration. Some of the methods includes Penman-Monteith (Penman,1948), Radiation method developed by Priestley and Taylor(1972), Radiation method developed Abteu and Melesse(2009),temperature and radiation method(Hargreaves et al., 1982).Even though there are several method used to determine the potential evapotranspiration in data scarce regions like Ethiopia it is a challenge to use data intensive models like Peneman-monteith. As a result choosing simple temperature methods in order to compute the ETO estimation based on single the temperature data was a primary choice in this study. Therefore a simple temperature method by Enku and Melesse (2014) was chosen to compute the evapotranspiration (Eqn 3.17).Estimated PET can be found under Annex A: 1.

$$ET_o = \frac{(T_{max})^n}{k} \text{ --- --- --- 3.17}$$

Where ETo is reference Evapotranspiration (mm/d), n=2.5 which can be calibrated for local condition and K is coefficients which can be calibrated for local condition.

$$K = 48 * T_{mx} - 33 \text{ --- --- --- 3.18}$$

Where T_{mx} is mean annual maximum temperature.

3.9 Sensitivity, Calibration and Validation HBV-96 Model

3.9.1 Sensitivity Analysis

Sensitivity analysis can help the modeler to determine which parameters sensitive to change the model output required. It helps to know which parameter is more sensitive in controlling the water balance (for HBV-96 case) and visualize the behavior of system being modeled, as well as evaluating the Performance of the model. Sensitivity analysis was conducted for the Megech watershed to determine which parameters are more sensitive to know the behavior of the model and evaluate the performance of the model. Another reason to do sensitivity analysis was in the hydrological modeling it is not possible to find one unique best parameter. This is due to different parameter set may give similar reasonable results during calibration. In order to reduce uncertainly and to define the optimum parameter set it was essential to do sensitivity analysis on model parameter (Wale et al., 2008).

3.9.2 Model calibration and validation

Usually water resource models include "free parameters," i.e. variables used in the mathematical formulation for which direct measurements do not exist. These can be estimated by adjusting their values until the resulting model prediction agrees with measurements; this process is referred to as model calibration. There are three major approaches for calibrating the model in order to identify the optimum parameter set. These include manual, manual and automatic and automatic calibration. Among these methods the manual calibration was applied for this study. This the calibration techniques by "trial and error" until the model yield better performance using the corrected parameter set. The performance of the model must be evaluated for the extent of its accuracy (Goswami et al., 2006). Hence, for this study, the model performance was evaluated during calibration and validation. This was carried out by inspecting simulated and observed hydrographs visually and using statistical model performance evaluation techniques such as Nash and Sutcliffe efficiency, coefficient determination (R^2) and Relative Volume Error (RVE). The Nash-Sutcliffe coefficient (Nash and Sutcliffe, 1970) is a measure of efficiency that relates the goodness-of fit of the model to the variance of measured data. NSE can range from $-\infty$ to 1 and an efficiency of 1 indicates a perfect match between observed and simulated discharges. NSE value between 0.9 and 1 indicate that the model performs very well while

values between 0.6 and 0.8 indicate the model performs well (A Wale et al., 2009). The largest disadvantage of this efficiency criterion is that larger value in a time series are strongly overestimated whereas lower values are of minor importance. For the quantification of runoff prediction this leads to an overestimation of model performance during peak flows and underestimation during low flow conditions.

The RVE can vary between ∞ and $-\infty$ but it performs best when a value of 0 (zero) is generated. Since an accumulated difference between simulated, Q_{sim} and Q_{obs} observed, discharge is zero. A relative volume error between +5% or -5% indicates that a model performs well while relative volume errors between +5% and +10% and -5% and -10% indicates a model with reasonable performance (Wale et al., 2009). Percent bias (PBIAS) measures the average tendency of the simulated data to be larger or smaller than their observed counterparts (Gupta et al., 2002). The optimal value of PBIAS is 0.0, with low-magnitude values indicating accurate model simulation. Positive values indicate model underestimation the bias, and negative values indicate model overestimation the bias (Gupta et al., 2002).

IJSER

Chapter Four

4. RESULT AND DISCUSSION

4.1 Land cover classification

4.1.1 Accuracy assessment

Accuracy assessment of image classification was done based on the observed ground truthing data to minimize error caused during land cover classification. A total of 200 ground control point were used to validate the classified image. The accuracy was performed for the 2015 image. This is because filed data was available only for 2015 site. The overall accuracy of the classification was 84 % with kappa coefficient of 83%. The kappa statistic was calculated from the result of the land cover classification, with five classes shown at the bottom of the error matrix table.

Table 4.9 Base Error Matrix of 2015 land cover class

classification	Reference data or ground truth classes					Row Total
	Open water	Built up	Agriculture	Forest land	Grass Land	
Open water	10	0	0	0	0	10
Built up	0	30	0	0	0	30
Agriculture	0	6	98	6	0	110
Forest land	0	0	16	20	0	36
Grass Land	4	0	0	0	10	14
Column Total	14	36	114	26	10	168

Table 4.10 Accuracy assessment of 2015 Land Cover class

Class Name	Reference Total	Classified Total	Number Correct	Producer's Accuracy %	User's Accuracy %
Open water	14	10	10	71.43	100
Built up	36	30	30	83.33	100
Agriculture	114	110	98	85.96	89.09
Forest	26	36	20	76.92	55.56
Grass Land	10	14	10	100	71.43
Totals	200	200	168		

For the average the user's accuracy is 83.22% and the average producer's accuracy is 83.53. The overall accuracy of the classification was 84 % with Kappa coefficient of 83%. The kappa value of 83% represents a probable 83% percent better accuracy. Monserud et al., (1992) recommended the Kappa value as <40% is poor,40-55% fair,55-70% good,70-85% very good and greater than 85% as excellent. Therefore based on above classification scale, the result of classification from this study could be considered as very good agreement. For the average accuracy and average reliability the results were 83.53 % and 83.22 % respectively.

4.2 Land cover classes

4.2.1 Land cover class of 1973

The land cover map and histogram of 1973(Figure4.10) indicated 55.56 % of the Megech sub basin was covered by forest land , 21.42% of agriculture land , 22 % by grass land and 0.07% was built up area. For 1973 land sate imaginary the land cover class (figure 4.11) showed that the Megech watershed was dominantly covered by forest land cover type.

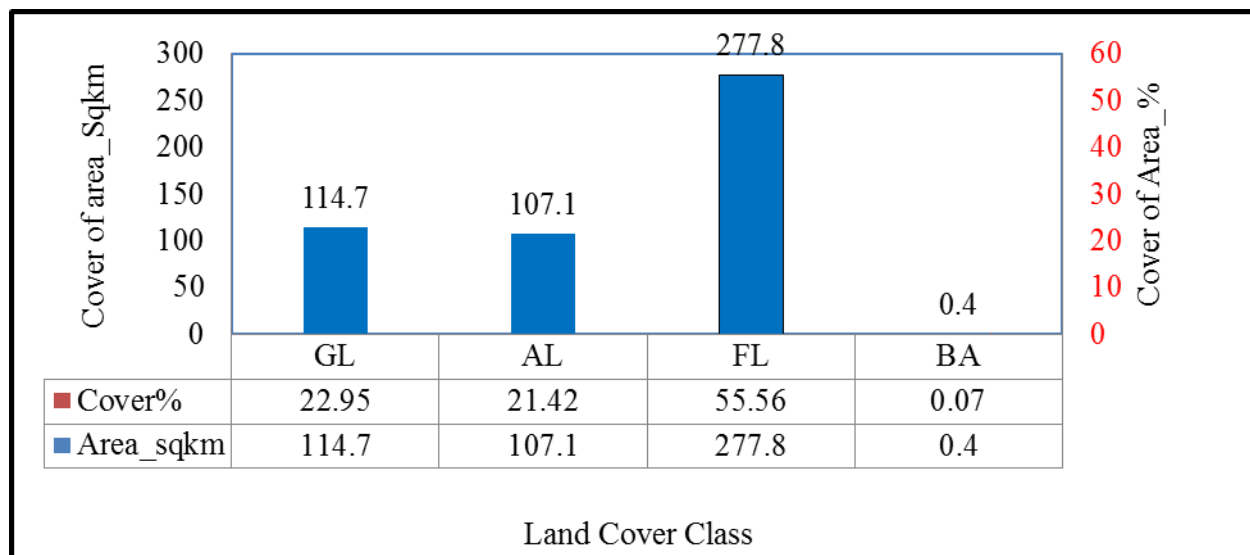


Figure 4.10 land cover class and relative coverage from 1973 Landsat image for Megech

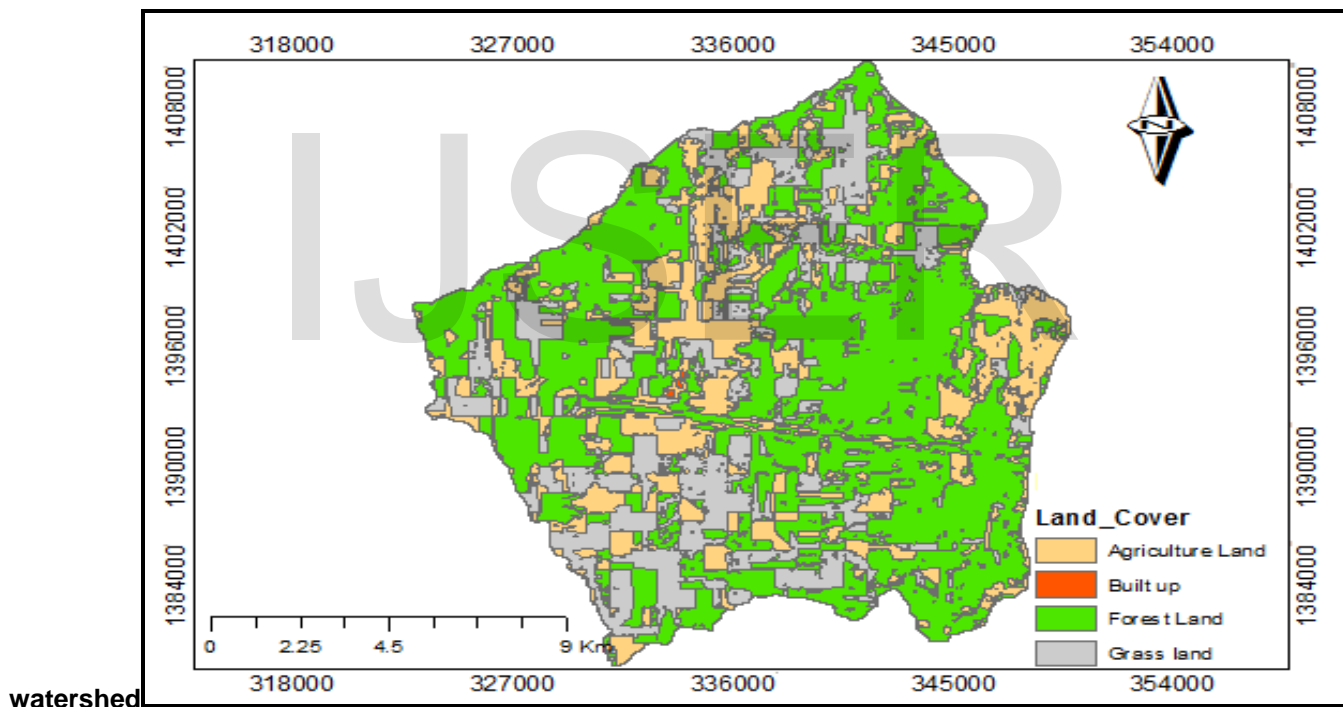


Figure 4.11 Land Cover map used as baseline and obtained from MoWIE for Megech watershed.

4.2.2 Land cover class of 1986

The land cover map and histogram of 1986 (Figures 4.12) showed 35.41% of the Megech sub basin was covered by forest land, 28.8% of agriculture land, 35.45% by grassland and 0.33% was built up area. The 1986 Landsat 5 image land cover class (Figure 4.13) showed that the Megech watershed was dominantly covered by Forest and grass land cover type.

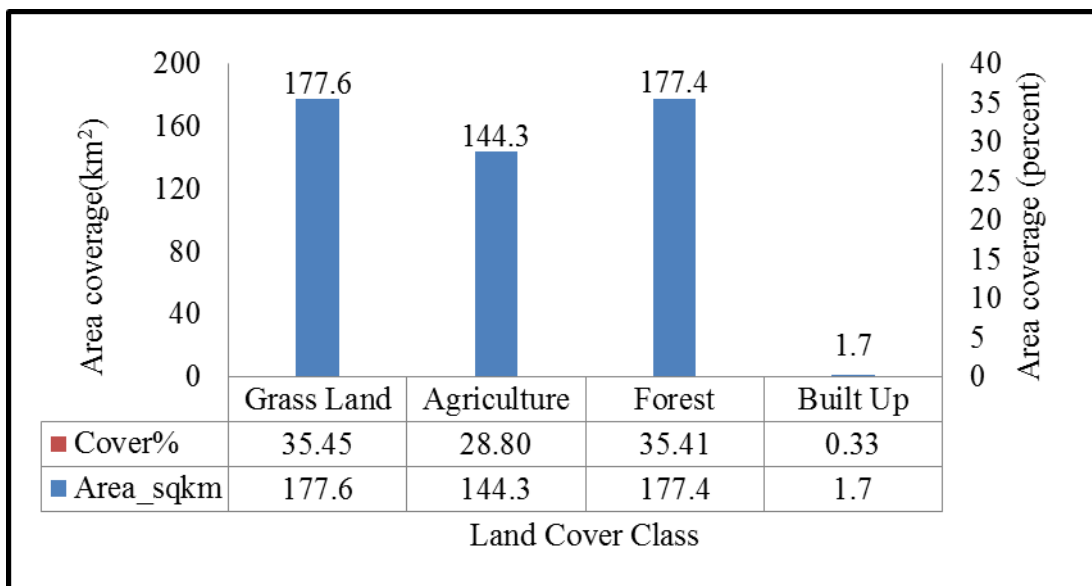


Figure.4.12 land cover class and relative coverage from 1986 Landsat image for Megech watershed

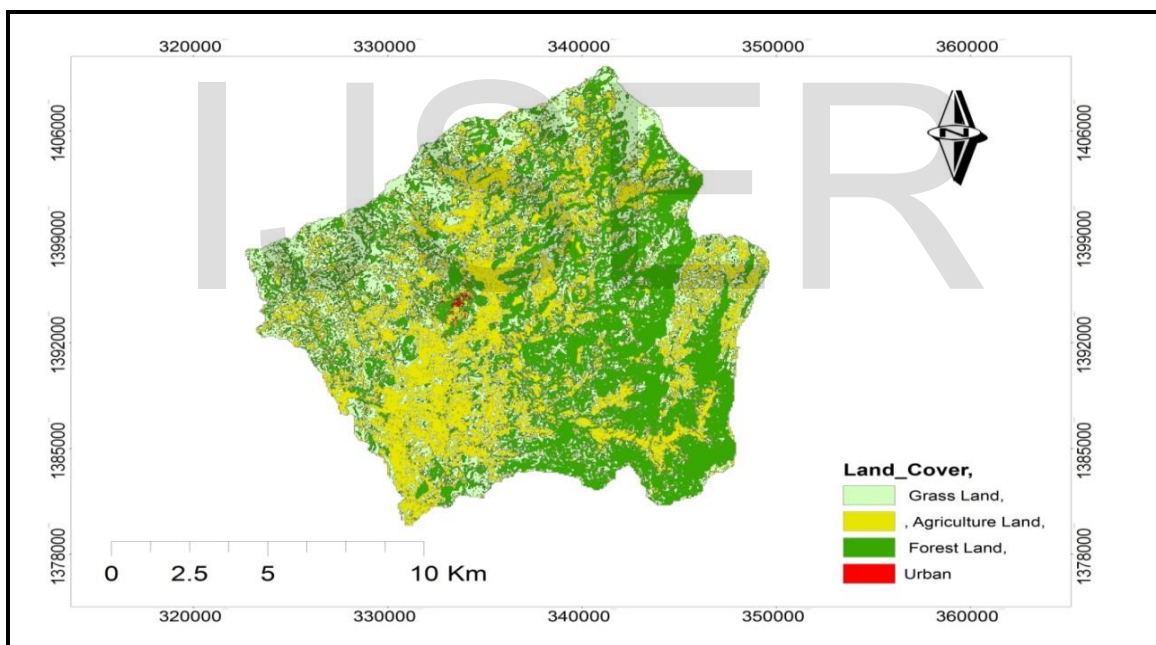


Figure 4.13- Land cover class and relative coverage from 1986 Landsat 5 image for Megech watershed.

4.2.3 Land cover class for 2007

The land cover map of 2007 and the histogram of the land class coverage (figure 4.16) showed that 77 % of the watersheds area was covered by Agriculture, 9% by forest land ,12% by grass and shrub land, and 2 % by built up area. The distributions of land cover class (**figure 4.17**) showed **Agriculture land cover was found in most parts of the watershed.**

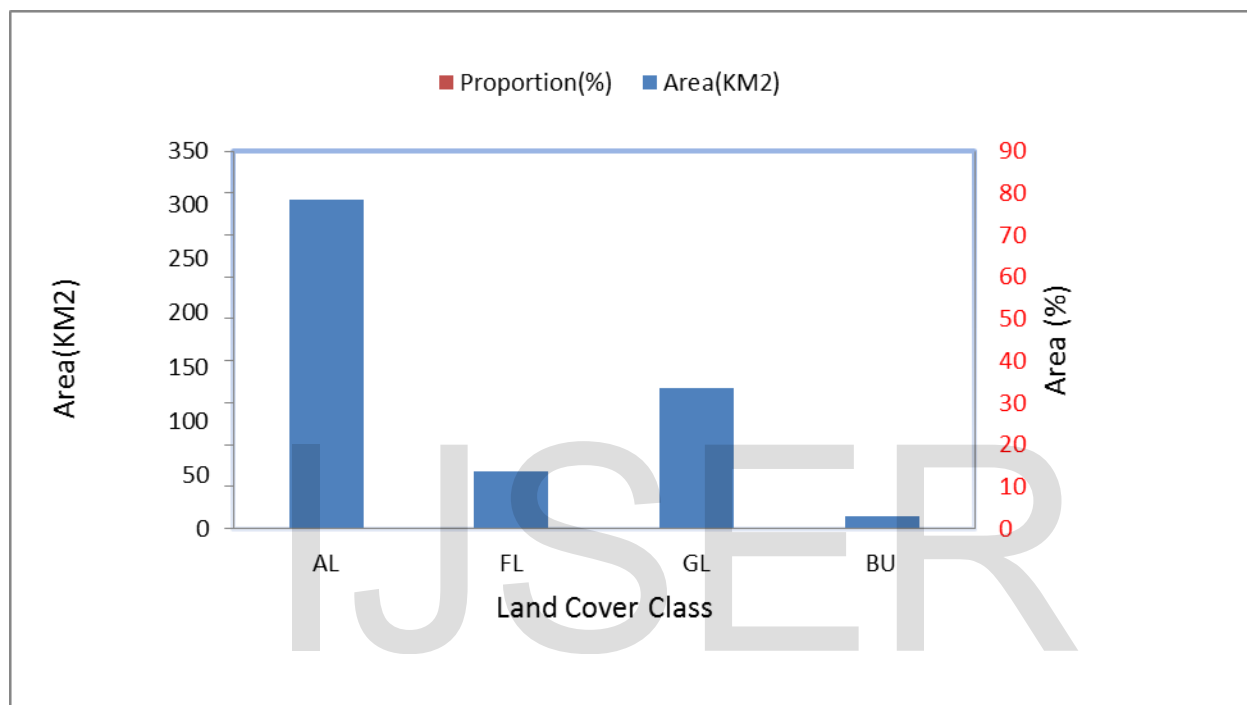


Figure 4.17 showed Agriculture land cover was found in most parts of the watershed.

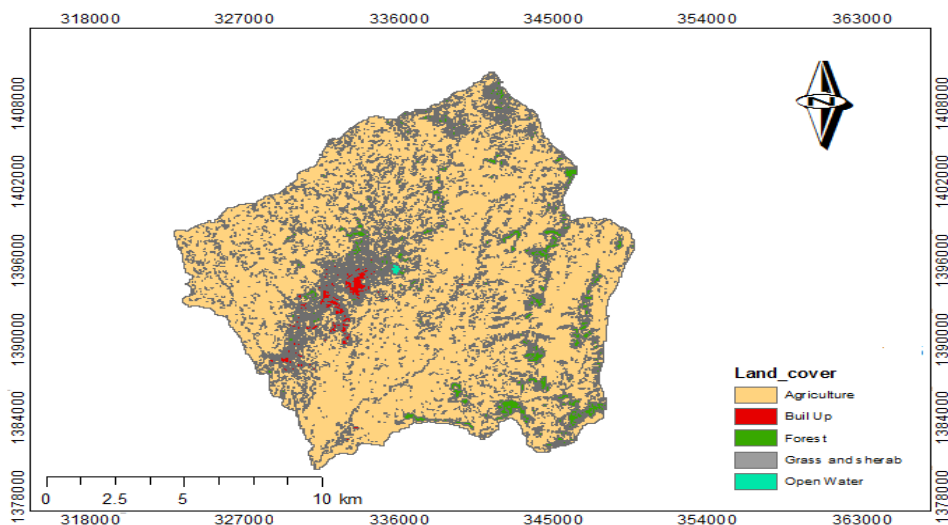


Figure 4.18- Land cover class and relative coverage from 2007 Landsat 5 image for Megech watershed

4.2.4 Land cover class of 2015

The land cover map of 2015 and the histogram of the land class coverage (figure 4.19)-showed that 88.6 % of the watershed was covered by Agriculture, 0.27 by Grass and shrub land, Forest land 7.79%, and 3.144% by built up area. The distribution of land cover class as it is shown in the below figure (4.20)

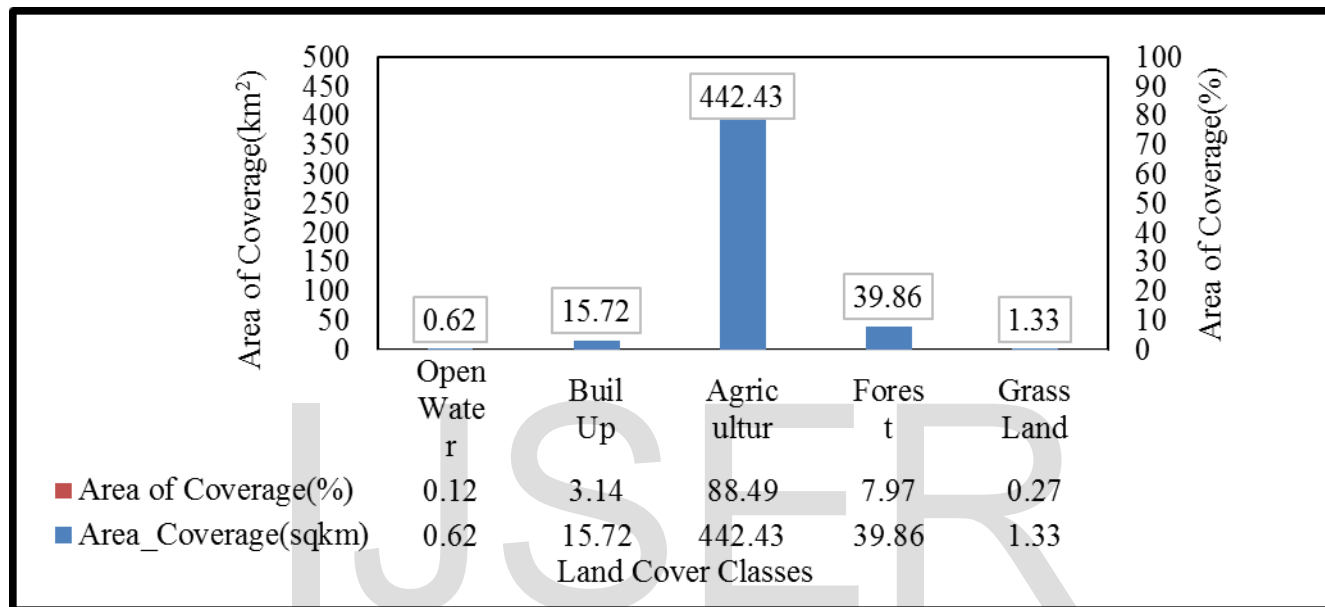


Figure.4.19 Land cover class and relative coverage from 2015 Landsat 8 image for Megech watershed.

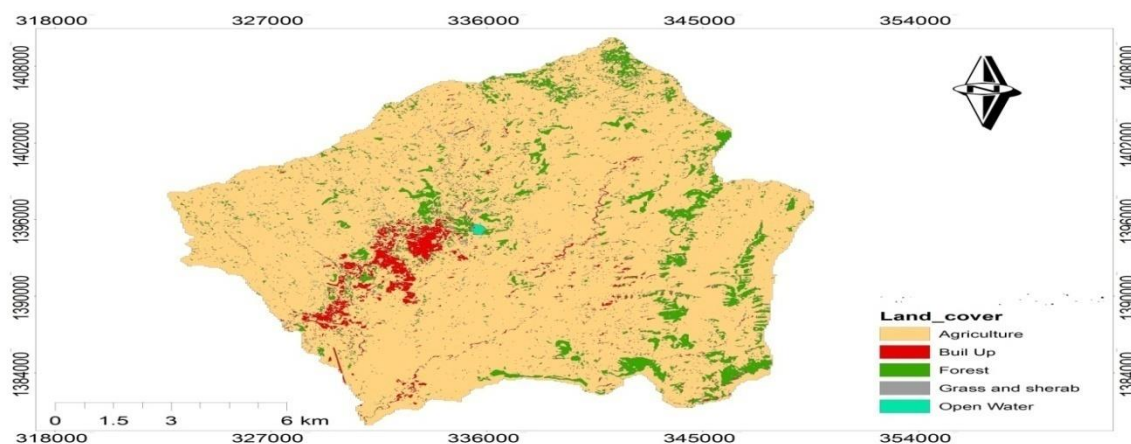


Figure.4.20 Land cover map of Megech watershed developed from 2015 Landsat 8 image

4.3 Trends in land cover classes (1973-2015)

In order to evaluate the trends of land cover classes’ Landsat images of three time periods (1973, 1986

and 2015).The analyses for each land cover class, for the period of 1973 to 2015 were summarized in the table 4.11 and figure 4.20.During the period of 1973-1986, agriculture land has increased approximately by the rate of change of 0.57% per annual. While area of the watershed covered by forest decreased by 20% with a rate change of 1.53% per annum. These changes showed that the deforestation has increased and covert the forest land into agricultural land. On the other hand during the periods of (1973-1986) the grass land coverage of the watershed was increased by 12 %.

Table 4.11 Land Cover class in Megech watershed (1973, 1986, 2015)

Land cover	Period of land cover class in Megech watershed(1973-2015)							
	1973		1986		2007		2015	
	Area	Proportion	Area	Proportion	Area	Proportion	Area	Proportion
	(Sq.km)	(percent)	(Sq.km)	(percent)	(Sq.km)	(percent)	(Sq.km)	(percent)
Agriculture	107.09	21	144.27	29	304	77	443	89
Forest	277.79	56	177.36	35	54	9	40	8
Grass	114.71	23	177.55	35	130	12	1	0
Built up	0.35	0	1.67	0	12	2	16	3
Total	499.94	100	500.85	100	500.0	100	500	100

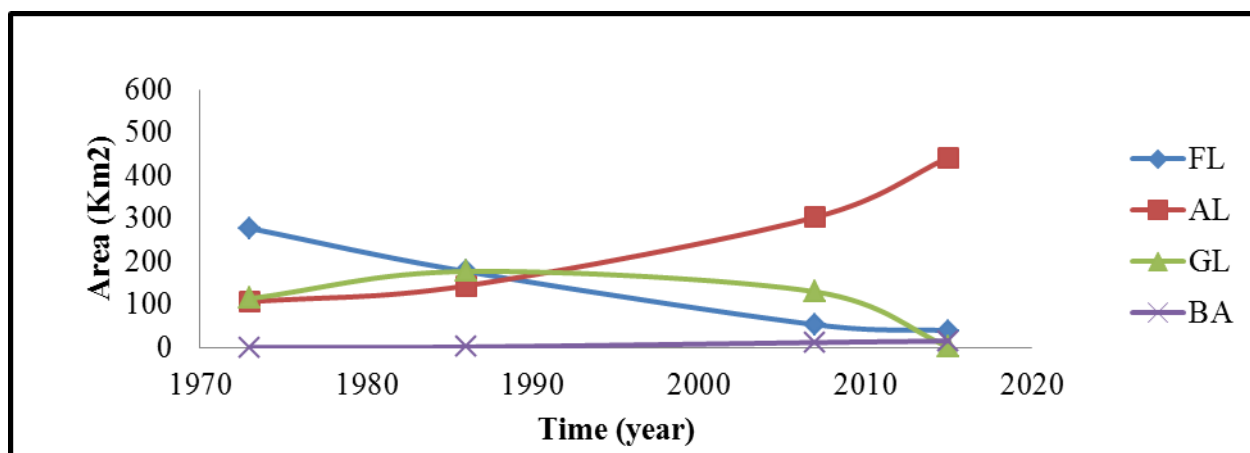


Figure 4.21 Land cover class trend analysis from 1973 to 2015

During the period of 1986-2015, the agriculture area in the watershed increased by 60% with an average rate of change of 2% per annum, while the forest decreased by 35% with an average rate of change of 1.217% per annum. Generally there is an increase in the water area in the watershed during (1986-2015). This was due to the establishment of man-made reservoir of Angereb dam (source of Gonder town water

supply). From 1973-2015 all of the agricultural expansion has resulted from the deforestation where forest lands are cultivated and become agricultural land. Therefore, in the year 2015 approximately 55% of forests were destructed in comparison to what it was compared with 1973.

The results of the statistical change analysis of the study area are shown (table 4.11). In the change detection analysis, it can be stated that a comparatively significant variation in land cover occurred between the years 1973 and 1986. Table 4.12 demonstrate the kind of land cover change, namely “from-to” information that occurred between (1973 -1986), (1986–2015) and (1973 – 2015) respectively. As it is shown in Table 4.12, 100.43km² forest areas was converted into agriculture land, Grass and Built up Area during the period 1973-1986.

The Grass land show in 1973 is 22%(114.71km²) ,that was expand in the period of 1986 by 35%(177,55km²) and reduced in the period 2015 by 0.27%(1.33km²). Similarly from the total of forest cover in the period 1973(277.79km²) of it was conserved; among that 62.84km² of it was converted into shrub land and 37.18km² to Agriculture. On the other hand, 1.32km² of built up area.

Table 4.12 Summery of land cover changed in different time periods in the Megech watershed

Period Interval	Land cover type	Agriculture	Forest	Grass	Built up
1973-1986	Change in area(km ²)	37.2	100.4	62.8	1.3
	Decrement (%)	-	20.1	-	-
	Increment (%)	7.4		12.6	0.3
1986-2007	Change in area(km ²)	-160.11	123.78	47.55	-10.33
	Decrement (%)		25	9	
	Increment (%)	32			2
2007-2015	Change in area(km ²)	138.67	13.69	128.67	3.72
	Decrement (%)		3	26	
	Increment (%)	28			1
1973-2015	Change in area(km ²)	335.96	237.9	113.38	15.37
	Decrement (%)	-	-48	-23	-
	Increment (%)	67	-	-	3

In table 4.12 the negative and positive sign indicates the decrease and increase of land cover class for the specified time period respectively. During the periods 1986 and 2015, the statistics provided in table 4.12 indicate that a total decrease of 137.47km² of forest and 176.22 km² Grass land was occurred; 298.78km² of it was converted to Agriculture land, 14.05km² to buildup. During the period (1973 to 2015) period of the study 237.9Km² (48% of the forest) area was decreased. 67% (335.96 km²) of the

Agriculture land was increased. By increase of population in the area there is also an increasing need to fire wood. As a consequence also the remaining forested areas became further under pressure.

4.4 Land Cover Trend Analysis for Last 10 years

Last 10 year study assumed year (2007) as bench mark for land use land cover trend analysis during 2007-2015. Ethiopian has been altering and facing problem starting from 1996 because various land use conflict arise from increased population number and human needs and change in land use admistration and policy. The trend analysis used for last 10 year as this much appropriate to obtained significant change in rural land uses. The comparison the land cover statistics assisted in identifying the percentage change trend the rate of change between 2007 and 2015 measured against each major land cover (fig 4.16). The factor influenced land cover change of the study area during the last 10 years imposed positive and negative impacts on land cover of the study area. In steep areas where closure area development exercised and trees were planted, soils were saved from being washed away and natural vegetation and fauna including grasses and trees were regenerated and as a result the downstream area is protected from flood hazard apart from the better income and benefits obtained in situ. On the other hand, trees planted around homesteads, along field boundaries and roadsides provide wood for household consumption and sale though they were competing with crop fields. In addition, conversion of hills, valley bottom, low-lying forest and grasslands into croplands reduce grazing land used by the people communally, resulting into reduction of the number of livestock per household and favor severe soil erosion and land degradation. However, it partially solved the problem of land shortage emanating from population growth and formation of new households. Illegal expansion of cultivated land on steep slopes covered with natural vegetation on the other hand caused degradation of biodiversity and enhanced soil erosion.

The ownerships and a good start has been observed in some highland area through privatization of communal land and use by cut and carry system. Free grazing is also a problem with crop cultivation and soil erosion control. In general, land cover changes in the forest area were quite significant. Consequently, the clearing of forest and the increase in agriculture land has resulted to gully erosion in several parts of the watershed as shown in figure 4.19.



Figure 4-22: Gully erosion in one of many locations of Megech catchment (Picture taken by Zemenu A. 2015)

4.4 Hydrological Modeling Sensitivity Analysis, calibration and validation

After the model setup has been completed the next step was to run the model and analyze the simulation results. The applicability of the model for intended purpose was evaluated through the process of sensitivity analysis, calibration and validation.

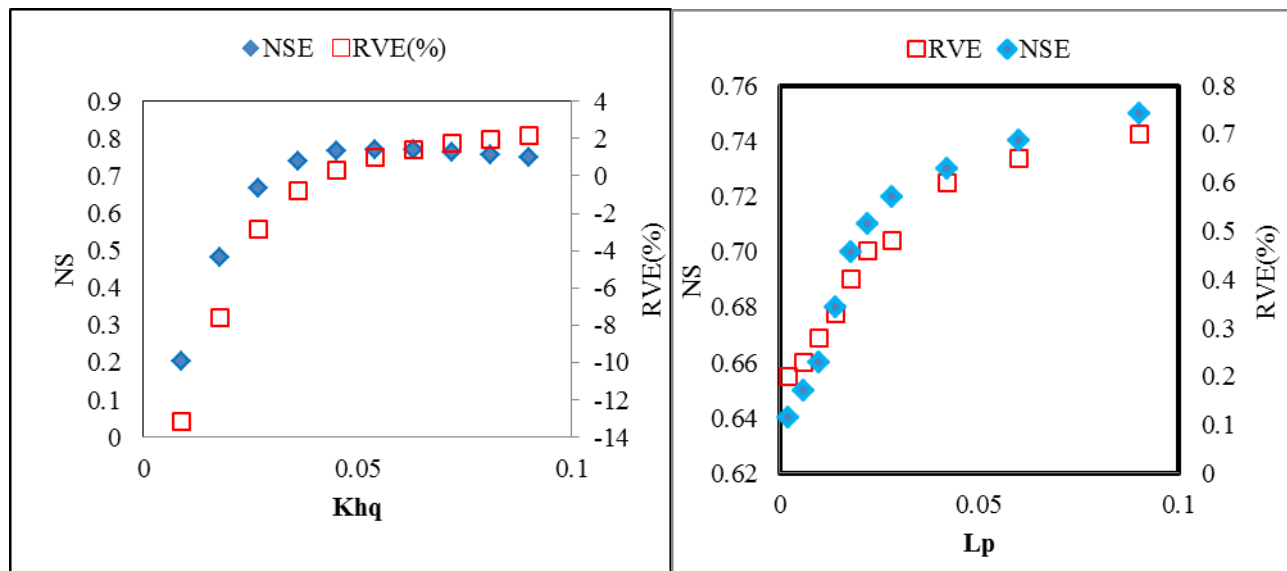
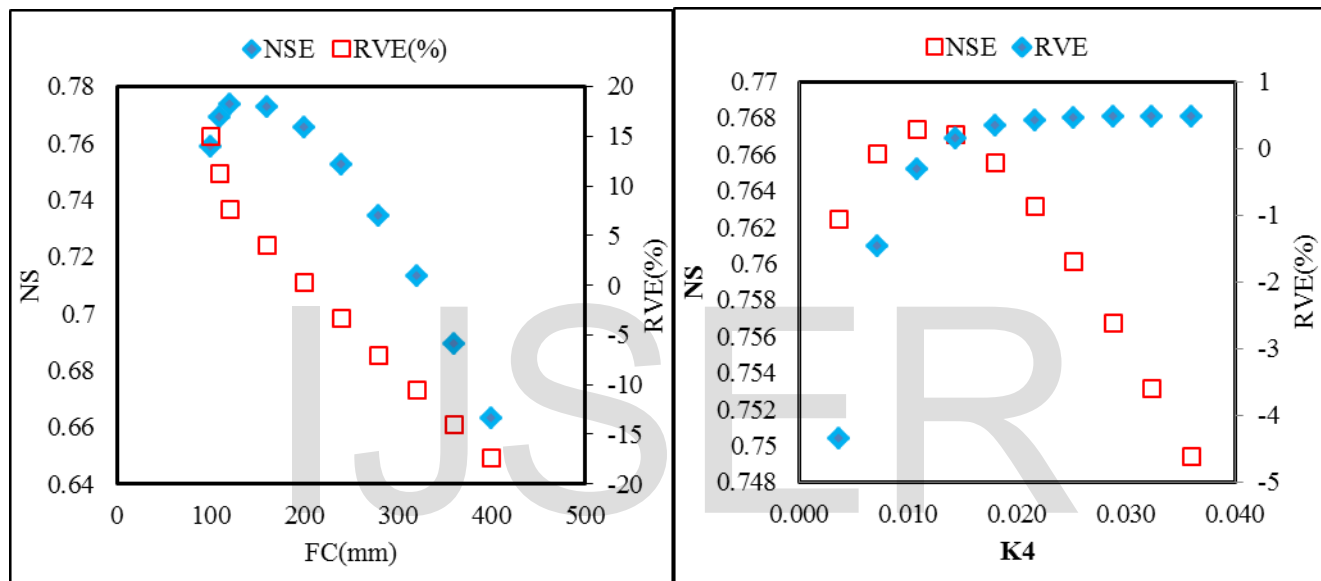
4.4.1 Sensitivity analysis

Sensitivity analysis was helpful to rank and identify the most sensitive parameters based on significant impact for each parameter. The most sensitive parameter corresponds to greater change in output response. This information is important during model calibration. In HBV-96 model there are seven model parameters controlling the total volume and shape of the hydrograph (Wale et al., 2009). The sensitivity and calibration of model was carried out based on these parameters. These parameters were divided into volume controlling (FC, LP, Beta) that influence the total volume and shape controlling parameters (K4, K, KHQ, HQ and Alpha) that distribute the calculated discharge in time and influencing the shape of hydrograph. In this study manual sensitivity analysis has been done by changing each parameter and keeping others constant separately within the ranges of the parameter. Result of the sensitivity analysis (table 4.14) showed that the KHq, FC, and LP were highly sensitive parameters of 21%, 17% and 39%. Other parameters were categorized also low to moderately sensitive (Beta, HQ and Perc). While Alpha (α) were found non-sensitive (Table 4.14, figure 4.20) showed the sensitivity parameter difference in % of volume and shape.

Table 4.13 Parameter range Values for HBV-96 model

Parameter	Description of parameter	Parameter Range	
		Minimum	Maximum
Alfa (α)	Measure of non-linearity to the response of upper reservoir	0.5	1.1

Beta	Exponent in the equation for discharge	1	4
FC	Maximum soil moisture storage	100	1500
KHQ	Recession coefficient for upper response box	0.0005	0.2
K4	Recession coefficient for lower response box	0.001	0.1
LP	Limit for potential evaporation	=<1	1
Perc	Percolation from upper to the lower response box	0.01	6



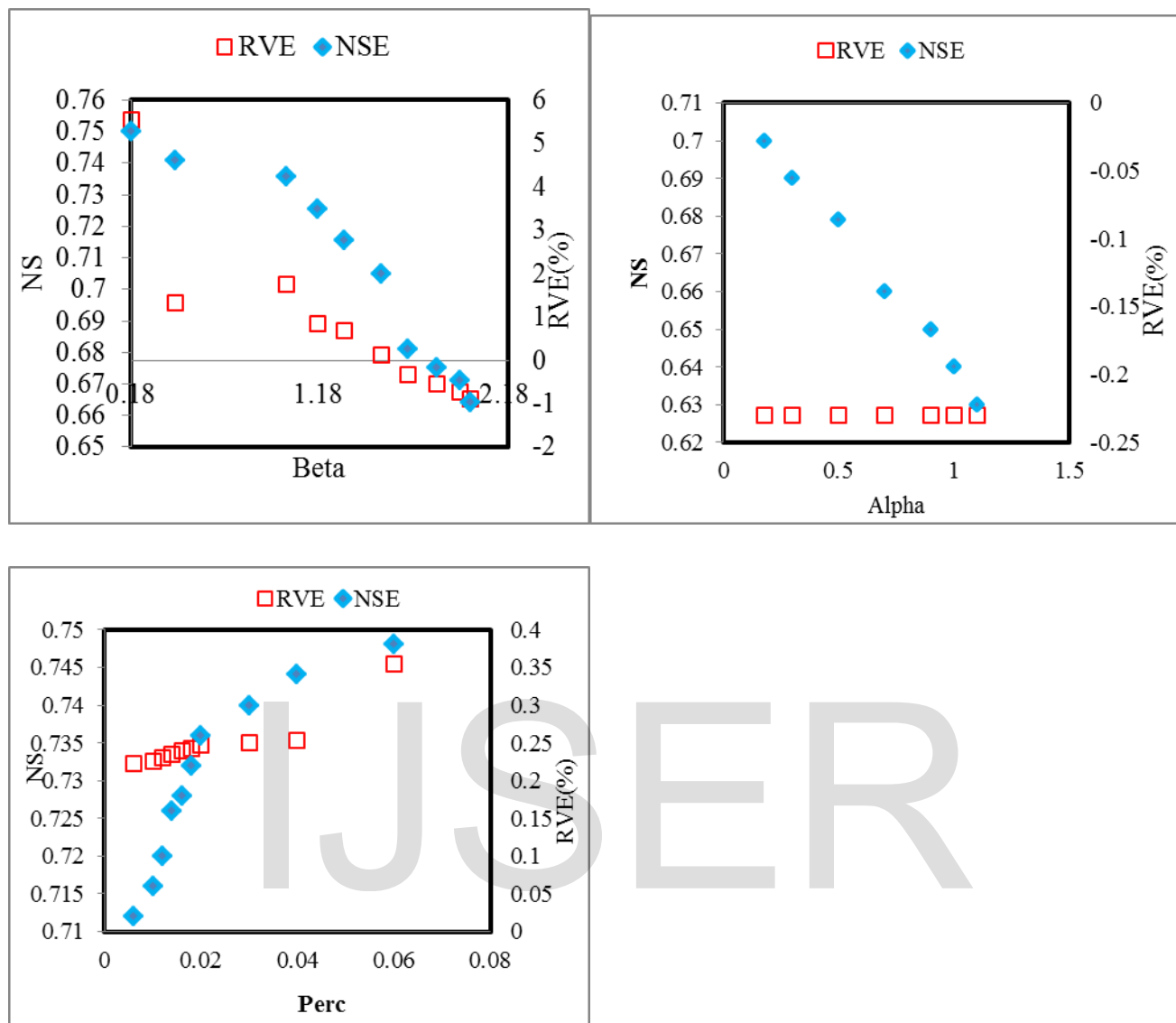


Figure 4.23 Sensitivity analyses for HBV_ model parameters evaluated in the relative change of evaluation criteria's in Megech watershed

Table 4.14 selected percent of difference Nash and RVE during sensitivity analysis

No	Parameter	Nash difference	RVE difference	Difference	Sensitivity Analysis rate	Rank
1	Alfa (α)	0.07	-0.18	0.25	Fairly sensitive	6
2	Beta	0.09	6	5.91	Moderately	5
3	FC	11	31.39	20.39	High	2
4	KHQ	0.6	-16	16.6	High	3
5	K4	0.06	-6	6.06	moderately	4
6	Lp	11	50	39	High	1
7	perc	0.04	0.1	0.06	Fair sensitive	7

The soil routine in the HBV model was governed by two relations (table 4.14) and the three parameters (f_c , l_p , β). At low soil moisture levels most of the precipitation is kept within the unsaturated zone. The share of precipitation contributing to the discharge increases gradually as the soil moisture increases as a bigger part of the area reaches its field capacity. This process is run by f_c and β . Response parameters: during calibrating the response parameters are, k_4 , $perc$, khq , hq and α . These parameters distribute the calculated discharge in time and thus are influencing the shape of the hydrograph but not the total volume (IHMS, 2005). As it was mentioned in the methodology (eqn 3.16) hq was not a calibrated parameter which was calculated from the catchment characteristics and provided the result as 5.755mm/day. The sensitivity analysis (table 4.14) depicted that l_p , f_c and KHQ were the most sensitive among the parameters identified to be used for calibration of stream flow in Megech watershed. The sensitive parameters obtained in this study were consistent with parameters identified by Wale et al., (2008) and Rientjes et al. (2011).

4.4.2 Calibration

As indicated in the methodology sections the data from 1986 -1991 was used for calibrating HBV96 model. Validation was performed from 1992-1995 for daily stream flow using the sensitive parameter identified. The flow was calibrated by using manual calibration with the observed flow at the outlet of Megech river. The manual calibration has been done by changing the parameters iteratively until the model efficiency falls in the acceptable ranges with the optimum parameter value. After calibration observed and simulated stream flow reasonably indicated an agreement with ($R^2 = 0.74$) as indicated in Figure 4.20. In addition to evaluation using the model efficiency criteria this hydrograph shows the model simulates the flow in a good manner compared with the observed stream flow data. The hydrograph with the baseline land cover showed good agreement in the base flow than the peak flow meaning the model over estimates compared with the observed flow.

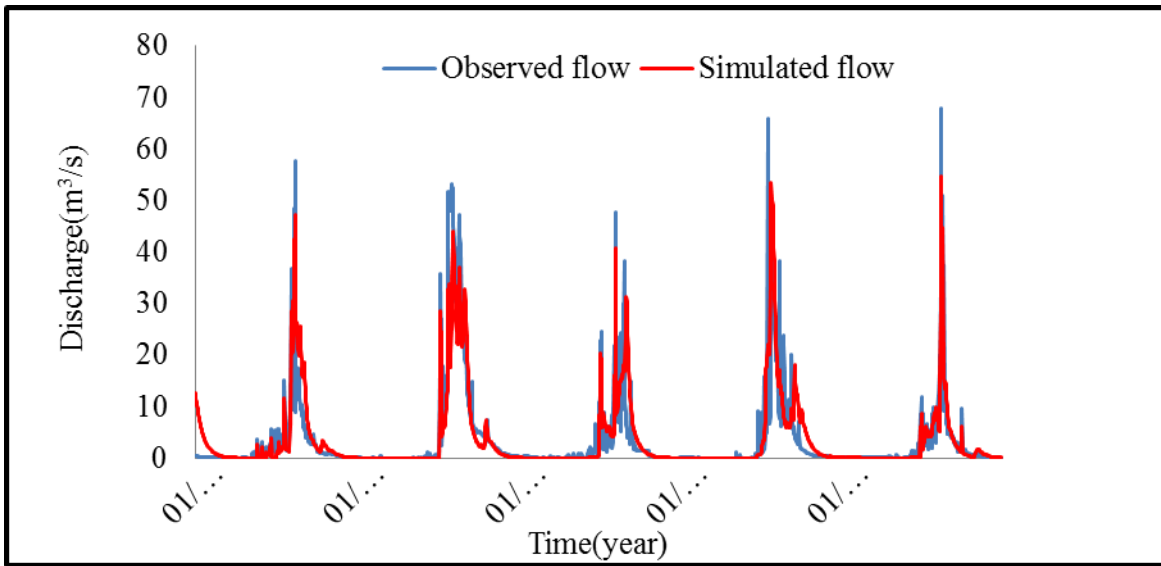


Figure 4.24 Simulated and Observed stream flow using baseline land cover for Megech watershed during calibration period.

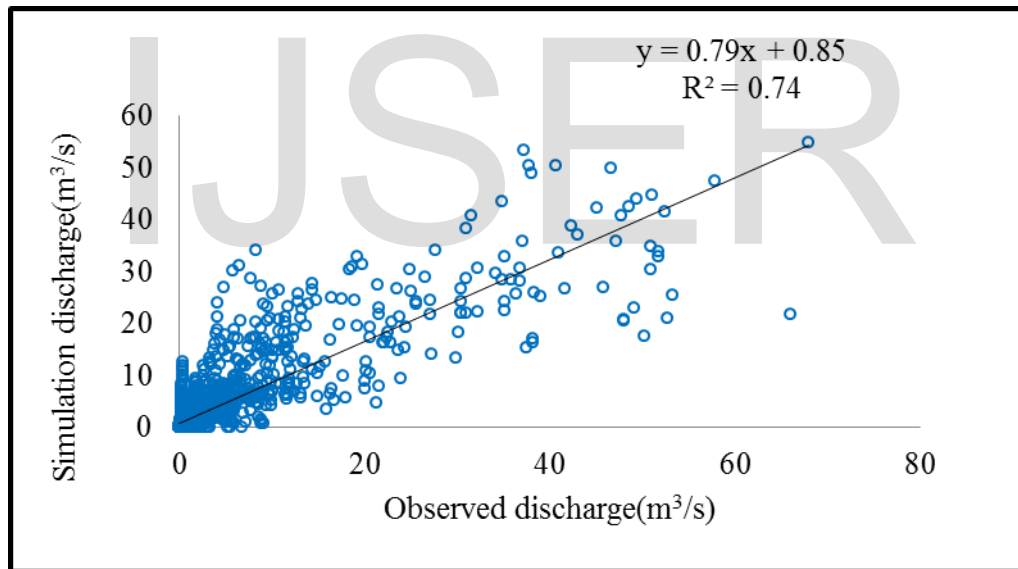


Figure 4.25 scatter plot using baseline (2008) land cover of Megech watershed for calibration period

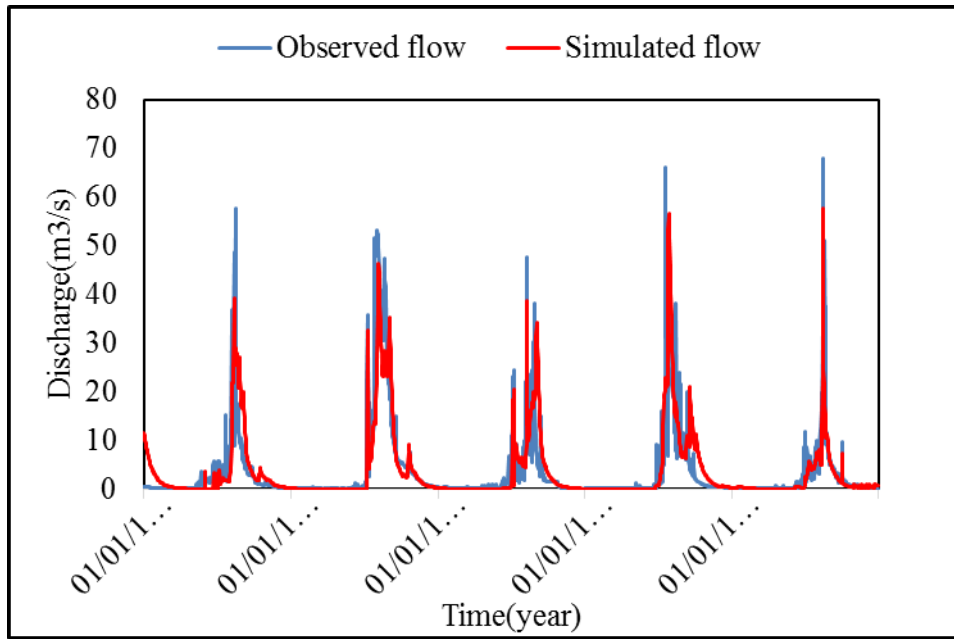


Figure 4.26- Simulated and Observed stream flow using 1986 land cover of Megech watershed for calibration period

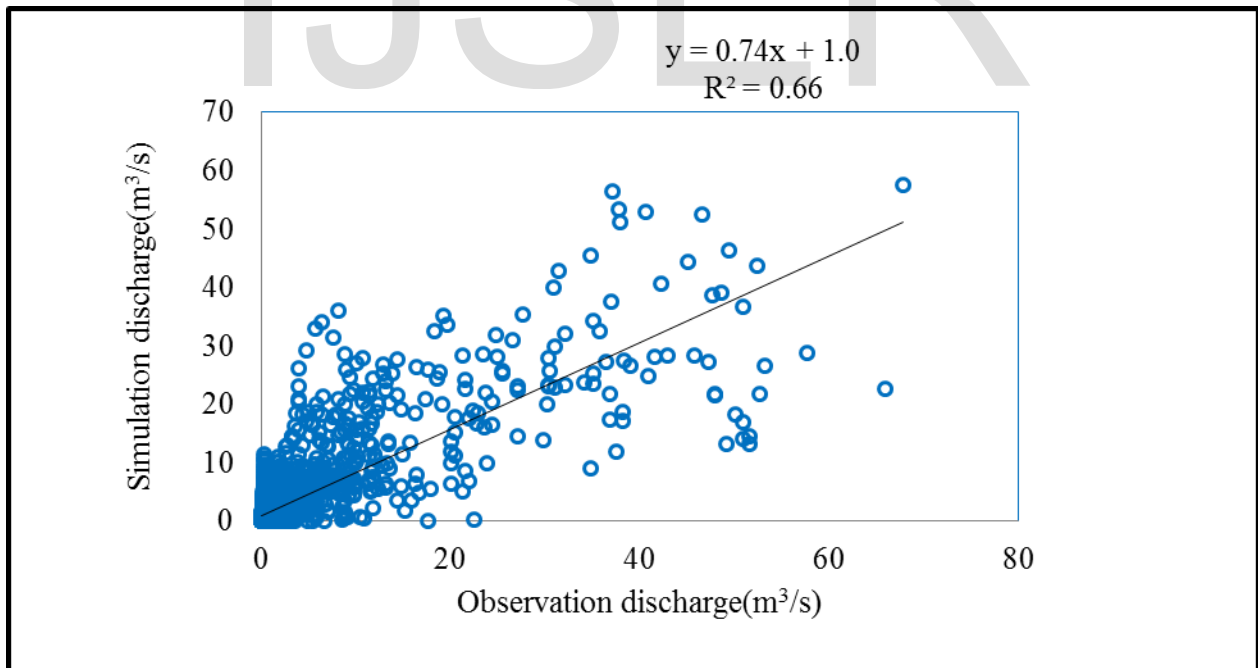


Figure 4.27scatter plot using 1986 land cover of Megech watershed for calibration period

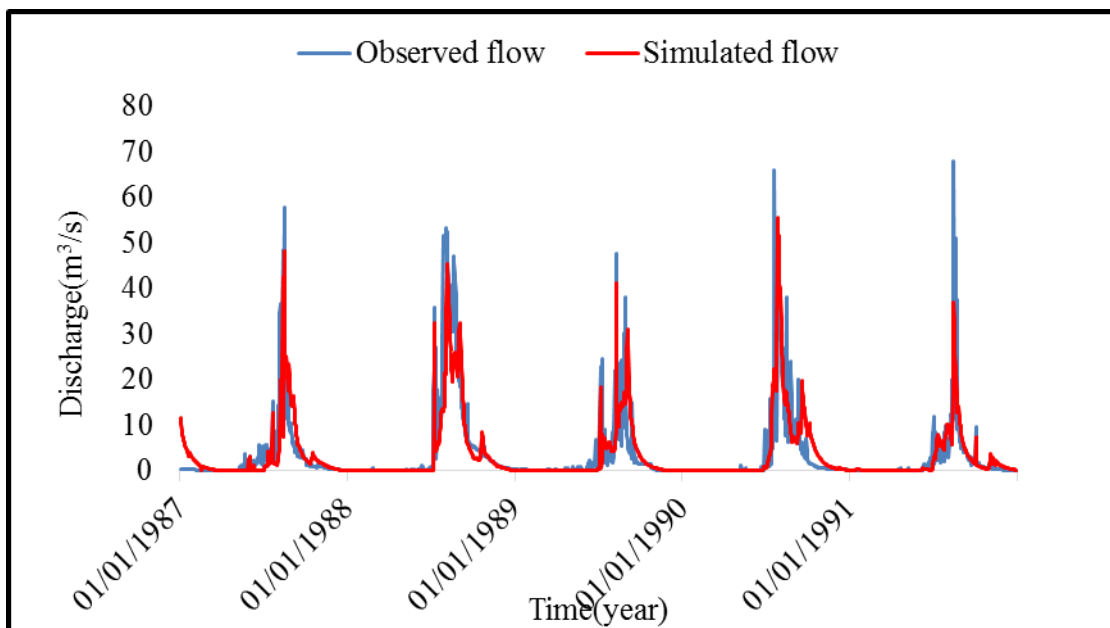


Figure 4.28- Simulated and Observed stream flow using 2015 land cover of Megech watershed for calibration period

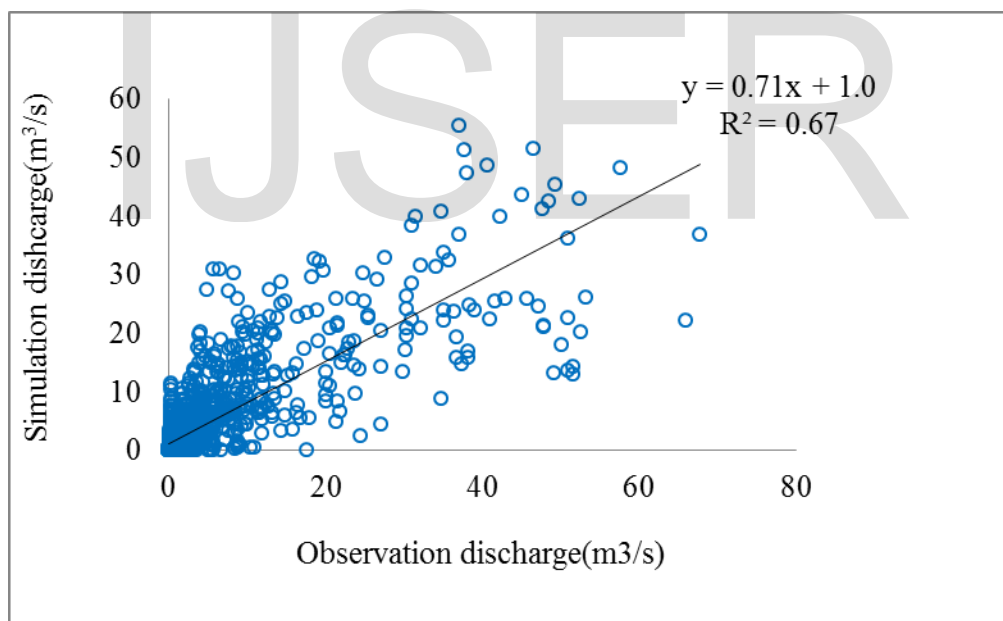


Figure 4.29- scatter plot using 2015 land cover of Megech watershed for calibration period

Rientjes al., (2011) found relatively high values for the 6 catchments with highest model performance value of 0.85 for the Gilgel Abay catchment but Megech watershed calibration NS value was 0.61 and RVE 2.91%. However in this study the calibration showed relatively high values using the land cover data of 1986, 2015, and Baseline(2008) with NS(=0.65,0.68 and 0.74) and RV(=3.9%,0.56% and 3.8%) respectively. The difference from previous study might be due to difference in station selection for rainfall and temperature data. The station used in this study was Shermbekit which have an aerial

coverage of 82% while Rientjes et al (2011) and Wale et al (2009) used stations outside the watershed (Makesegnet, Tikeledenegay and Gonder). However, Haile et al. (2011) have also indicated that large topographic variability directly affected the rainfall patterns in Blue Nile Basin meaning that stations outside the watershed might not represent the rainfall characteristics in the watershed. In addition Megech watershed is relatively small in comparison to Blue Nile basin which would have similar characteristics in topographic variability directly affected the rainfall patterns. Therefore, the station used in this study were better represented the watershed and improve the model performance.

4.4.3 Land Cover change Induce parameter changes

During calibration using the the sensitive parameters with their optimum parametric value have taken to simulate the flow using the 1986 and 2015 land use data classified using the ERDAS Imagine. The parameter values optimized during calibration was changing during the simulation by the other land cover. Forexample (in Table 4.15)the soil storage capacity of the watershed showed a decreasing trends fc (422 and 279) for land cover shift from (1986 to2015). This showed that the change in land cover affects the evaporation amount in watershed.

Table 4.15 Land cover induce change for 1986 and 2015

Parameter	1986 LC	2007	2015 LC
	Optimum calibrated value	Optimum calibrated value	Optimum calibrated value
Alfa (α)	0.23	0.19	0.15
Beta	0.25	0.21	0.16
FC	430	350.00	270
KHQ	0.04	0.35	0.65
K4	0.003	0.001	0.002
Lp	0.026	0.25	0.50
perc	0.5	0.38	0.25

First the calibration processing has been done using the1986 land cover obtained at period of (2007 and 2015) flow was simulated. During shifting land cover type after calibration there was also shift in the parameter value which obtained during the first calibrated values. The simulations using the two land cover data of (2007 and 2015) resulted a parametric value shift from the 1986 parametric values optimized during the calibration. In Table (4.15) showed potential evaporation value was increased from 0.026 in 1986 to 0.50 in 2015 land cover change .example perc in 1986 was 0.5 and decreased to 0.25 in

2015 this might due to the land cover change resulted less water to infiltrate as most of forest land has been converted to agriculture there will be less residence time for the water to percolate and even the existing under such conditions was exposed to evapotranspiration

Recession coefficient for lower response box (K4) is parameters which have direct relationship with lower reservoir out flow. As indicated in the table for 4.15 it decreased from 0.003 using 1986 to 0.002 using 2015 land cover. This strongly indicated land cover change from 1986-2015 has significantly affected storage of lower reservoir or base flow of the watershed. Which by large indicated that increased of evapotranspiration due to land cover change. This might affect the already constructed Angereb reservoir for Gonder town water supply and planned Megech irrigation reservoir. This study showed that land cover change on the watershed resulted in change on the parametric values which characterizes the watershed including affecting the flow. From this effect we can understand that the land cover change have also the influence on the stream flow of the Megech river in one way or the other.

4.4.4 Validation

To ensure model performance independent data set from 1992-1995 has been used. The performance rating obtained was good and the model is applicable for assessing the land cover change impact on the stream flow of in Megech watershed. The calibrated parameters were validated through an independent set of flow data during the period of 1986, baseline (2008), 2015. The overall efficiency of the model that is evaluated by NS (0.64, 0.65 and 0.71) and RVE (-0.43, 0.040 and 0.37) value in the period of 1986, 2015 and baseline (2008) land cover change respectively during the validation period. These values reveal that the model results are satisfactory for this study

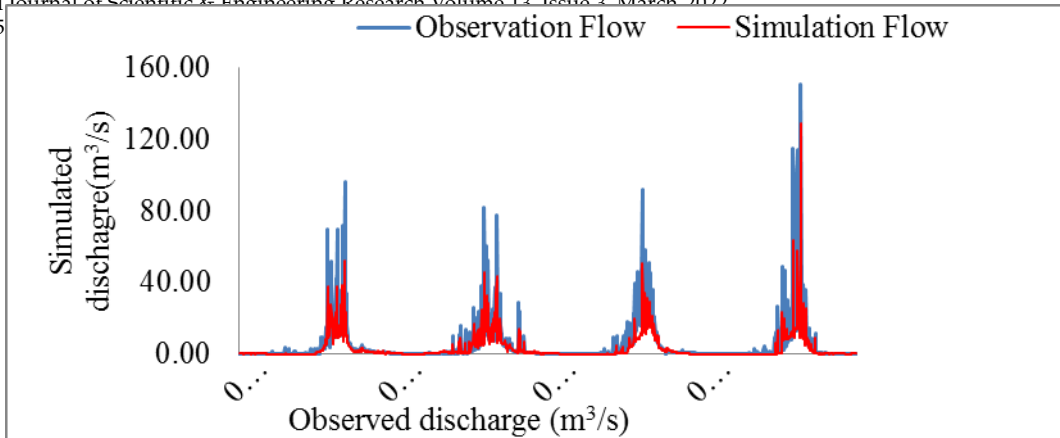


Figure 4.30 Simulated and Observed stream flow using baseline land cover of Megech watershed for validation period

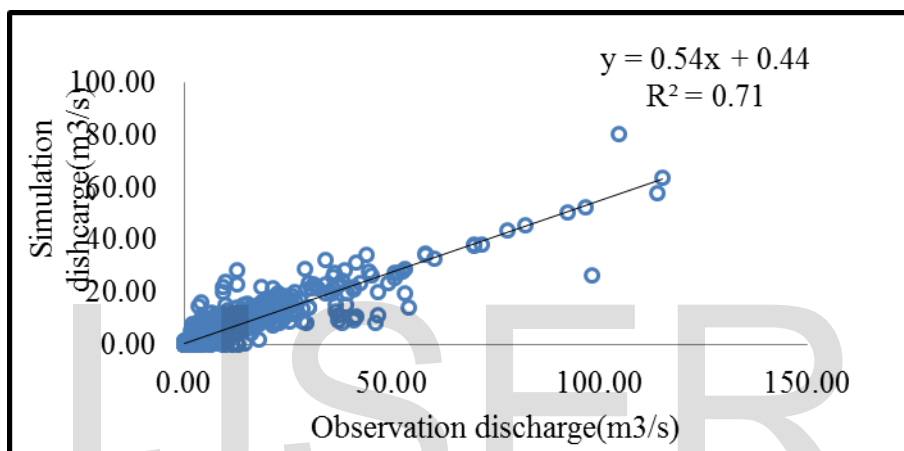


Figure 4.31 scatter plot using baseline land cover of Megech watershed for validation period

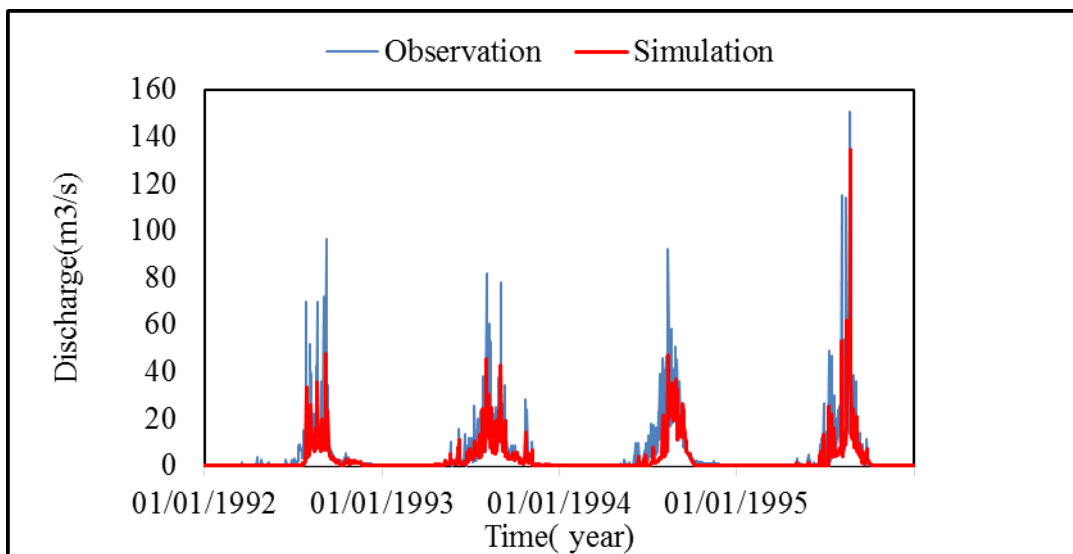


Figure 4.32 -Simulated and Observed stream flow using 2015 land cover of Megech watershed for validation period.

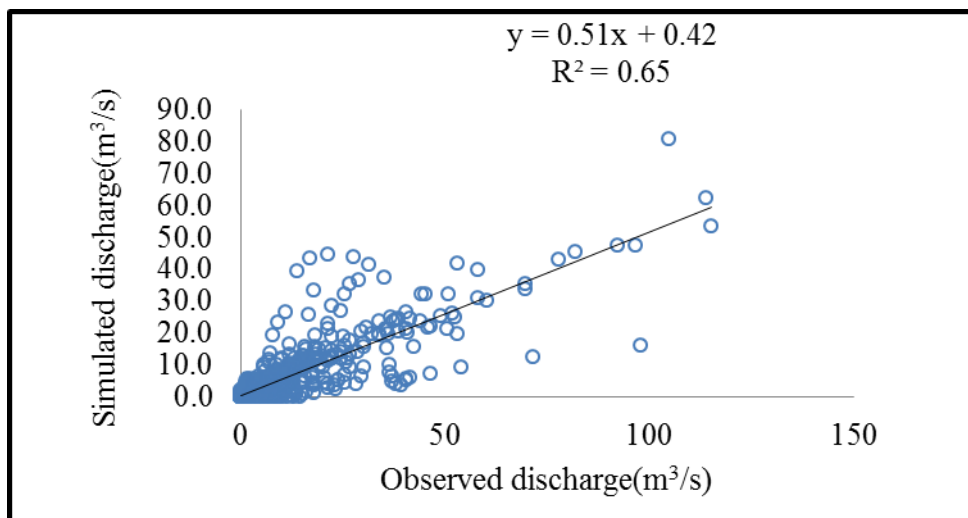


Figure 4.33–scatter plot using 2015 land cover of Megech watershed for validation period

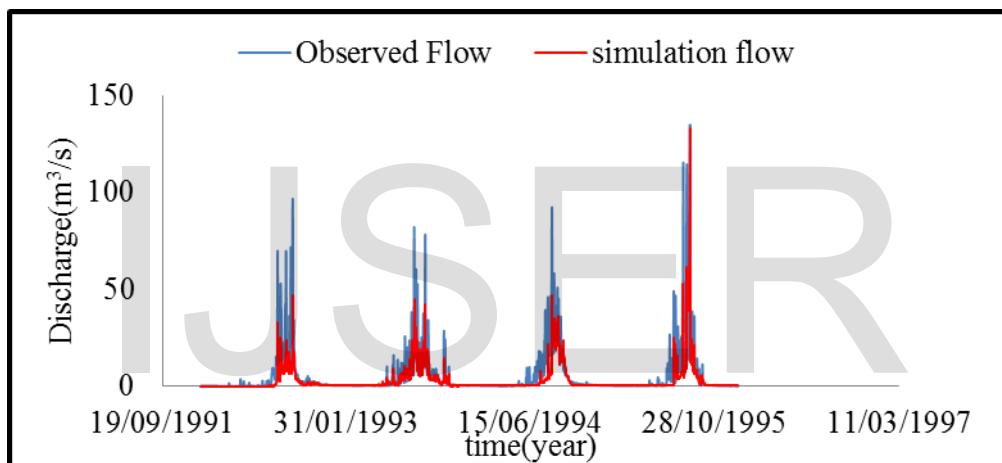


Figure 4.34-Simulated and Observed stream flow using 1986 land cover of Megech watershed for validation period.

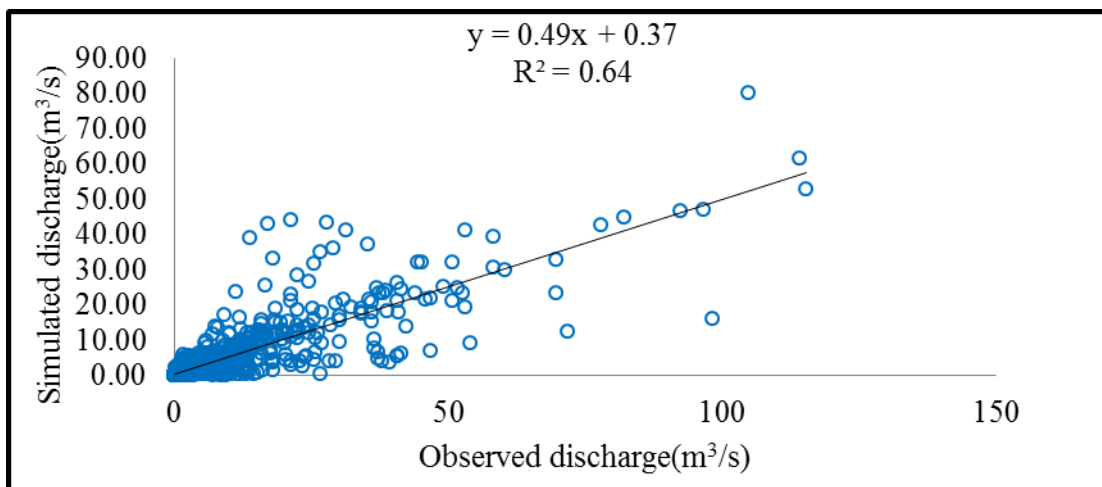


Figure 4.32-scatter plot using 1986 land cover of Megech watershed for validation period

Table 4.16 summary of the result of calibration and Validation

Parameter	Calibration(1987-1991)			Validation(1992-1995)		
	1986	2015	Baseline (MoWIE)	1986	2015	Baseline (MoWIE)
R ²	0.66	0.69	0.75	0.64	0.65	0.71
NS	0.66	0.68	0.74	0.64	0.65	0.71
RVE	3.9	0.56	3.8	-0.43	0.040	0.37

4.4.5 The effect of Angereb dam on Megech river flow

Angereb dam is constructed for water supply of Gonder town in 1986 on Angereb River, a tributary of the Blue Nile in the Ethiopian Highlands. Angereb watershed is characterized by hilly topographic conditions, absence of vegetation cover, improper farming and soil management practices (NBCBN, 2009). Therefore, Angereb river catchment experiences severe soil erosion which contributes to reservoir sedimentation and affects its water supply potential. To analyze the effect of this dam to downstream Megech river flow was taken for 26 years of the data of Megech River near Azezo (12.48° North, 37.45° East) having a watershed area of 500 km² of before and after construction of Angereb dam. The gauging site has no low flow control. The high flows usually are overtopping the river banks and usually are hard to be correctly estimated.

4.4.5.1 Before Angereb dam construction (1973-1985)

In order to analyze the changes in Megech river flows during the period (1973-1985) data was considered as before Angereb dam construction. The mean annual flow at the Megech dam site is found to have a value of 198 Mm³. Annual maximum Flow of Megech River at the gauging is 324 Mm³ as table 1.

4.4.5.2 after dam construction (1986-2001)

Megech river flows during the period (1986-2001) data were considered as after Angereb dam construction. The mean annual flow at the Megech dam site is found to have a value of 189 Mm³. Annual maximum Flow of Megech River at the gauging station is 189Mm³ as shown in table 1.

Table 4.17 Megech river discharge before and after dam construction

Period	Total Discharge (Mm ³)	Annual Discharge (Mm ³) maximum	Annual Discharge (Mm ³) minimum	Mean annual flow (Mm ³)
1973-1985	2573.4	324.5	1	198
1986-2001	2455.6	294	0.2	189
Difference	117.8	30.5	0.8	9

Generally, hydrological investigation with respect to before and after Angereb dam construction change within Megech watershed showed that the river flow regimes have changed, with decreased total discharged in the period of (1986-2001) due to Angereb dam construction.

Accordingly UNESCO (isi), 2008 and other studies have shown that the reservoir half life would be alarmingly about 21 years. According to their prediction the reservoir lost 15% of its volume in 2005 and would lose about 30% in the year 2015. The water resources verification study carried out by MoWR revealed that by the end of 2010 there will be shortage of water in Gonder town because the reservoir capacity will become less than 50% (from 5Mm³ to 2.5Mm³) as a result of sedimentation. This will definitely have negative impact on the people livelihood. Show data below table 2 (source: UNESCO, 2008).

Table 4.18 Angereb dam data (source: UNESCO, 2008)

Reservoir	Year of construction	Original capacity (C) Mm ³	Estimated loss (%)	Mean annual rate of sedimentation	Total Inflow (I) Mm ³	C/I	Brune Trap efficiency
Angereb	1986	5.25	15	1200 ton/km ² /yr	27	0.1852	90.23

Generally Megech river flow decreased after dam construction due to the two reasons the first the reason is due to Angereb dam construction and second reason is rainfall amount is decreased.

4.4.6 Effect of rainfall on Megech watershed

The analysis was dividing flow into two year's period were obtained ranging from (1973-1985) and (1986-2001) was done in order to get rainfall for a long time (26 years period) as presented in Table 3.

The rainfall of the same periods also was used to find the effect of rainfall contributes in watershed to various flow processes. The average daily rainfall data were 1136 mm in period of (1973-1985) and 1065 mm in period of (1986-2001). Therefore effective of rainfall in table 3 indicating that the total rain fall was decreased in the period of 1986-2001 than from (1973-2001) due to may be climate or other.

According to Weng (2001), there is close relationship between the change in land cover into runoff generation processes. The major relationship between land use and land cover change

(particularly reduction of tree canopy) causes more amount of effective rainfall to result on over land flow during the rainy season . This indicates that there is an interaction of the land cover and rainfall in determining the hydrological response.

Table 4.19 trend of annual rainfall (1973-2001)

Period	Total Rainfall (mm)	Mean annual Rainfall(mm)
1973-1985(before)	14765	1136
1986-2001(After)	13848	1065
Difference	916	70

The results displayed in figure1indicating the relationship between Megech river flow and rainfall during 1973-2001 .This revealed by average river flow decreased by 5% from 1986 to 2001 due to Angereb dam construction and rain fall amount was decreased.

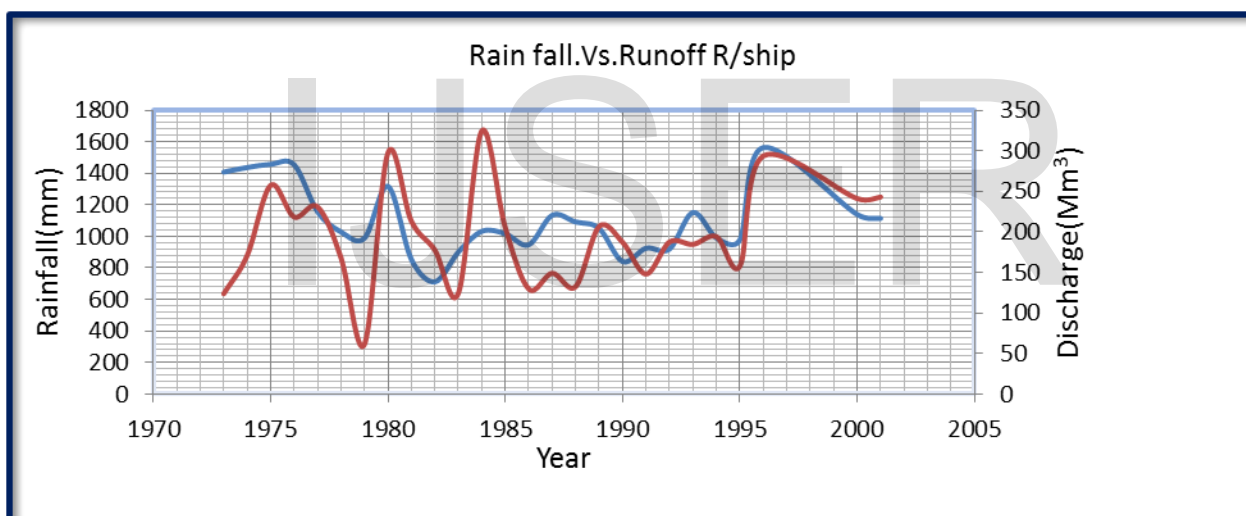


Figure 4.35 relations of Rainfall and runoff

4.4.7 Land cover change effect on Low flow

The low flow of any watershed has usually been recorded during dry seasons from February up to March mostly in our country Ethiopia (Woldeamlak Bewket, 2004). In this study area the annual minimum flow 1987-1995 years of periods was identified and the flow variation because of land cover change has also been evaluated. The 7day sustained low flow in a given year from the lowest flows was selected to represent the low flow in each year.

Generally the variation in low flow (Figure4.28) can be the result of land cover change in Megech watershed which has increased since 1986 for the reduction of base flow or low flow of the watershed.

The change in mean value of annual minimum flow has indicated a reduction of $0.06\text{m}^3/\text{s}$ which is 17% in 1986 to 2015 land cover. The annual low flow values were selected from the above two decadal periods 1986s and 2015s from already generated flow by land cover change of the watershed. As the result indicated, most of the area of the catchment has been covered by Agriculture land. This is due to agricultural expansion and consequently the other land cover classes had severely been depleted. Especially the forest and bush land classes which are very important physical catchment characteristics to reducing the overland flow and soil erosion of the catchment have been degraded. Currently these two land cover classes have covered very small areas i.e. 0.27% in forest and 7.9% in grass land respectively of the total area of the watershed. Due to this, the low flow trend of the catchment is decreasing (Figure 4.33).

The overall gap of these two curves in figure 4.33showed the decreasing trend of low flow because of land cover change of the watershed. The result indicates that the degradation of vegetation or expansion of agricultural land has been considerably affecting the environmental flow of the watershed. The decreasing of environmental flow has also been affecting the socio-economic situation of the study area. In terms of magnitude, the result has also been evaluated to quantify that exactly how much the land cover change has been affecting the low flow trend of the watershed.

Generally, a total recording period from (1987-1995) stream flow volume was decreased by 27%.The peak flow increased by $0.34\text{ m}^3/\text{s}$ and the base flow in the dry season also decreased by insignificant changes during the first period. For the record period the peak flow increased by (31%) while base flow decreased by 38% in 1986 to 2015 of the land cover change.

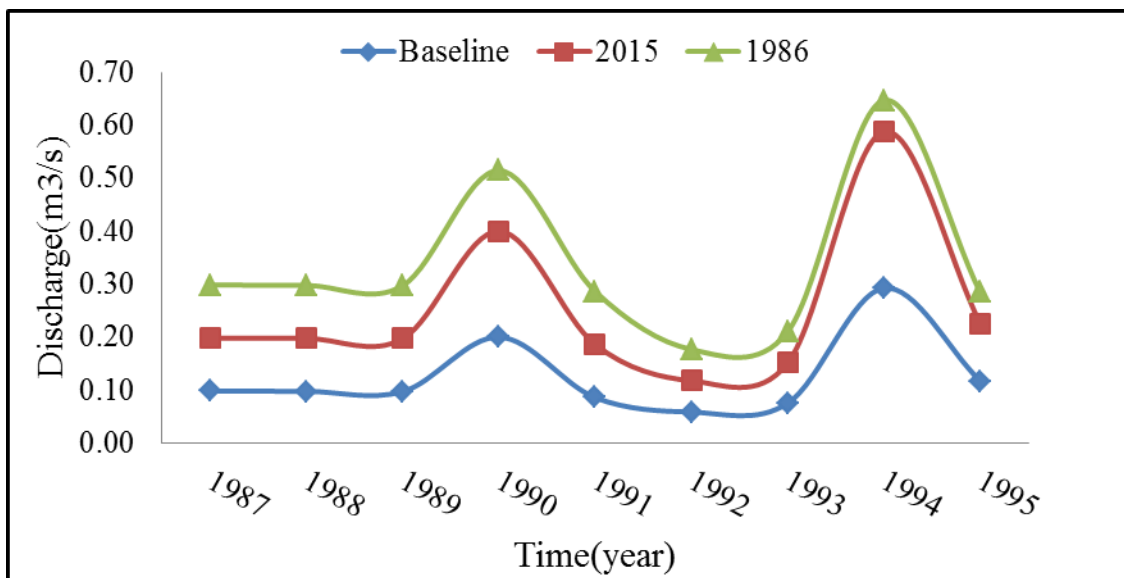


Figure 4.36 Observed and simulated low flows by using different period land cover maps baseline, 1986 and 2015

4.4.8 Flow Duration curve

Based on the available information on the land cover of the catchment, the stream flow data were analyzed based on the results of probability of exceedence for the periods (1986-1995) corresponding to 1986 and 2015 by compared with baseline land cover classes.

A five % exceedence probability represents a high flow that has been exceeded only 5-percent of all days of the flow record. Conversely, a 95-percent exceedence probability would characterize low-flow conditions in a stream since 95 percent of all daily mean flows in the record are larger than that amount. For this study, a 95% and 5% probability of exceedence was chosen to represent the minimum and maximum flow respectively. The results of this procedure are presented in (figure 4.34).

For 1986 land cover simulated flow the duration curve, showed the high flows exceeds by 5% up to 25% (figure 4.34). During the second simulated land cover 2015, peak flow analysis showed that the stream flow further increased by the rate of change of 0.57 m³/s, where as in the low flow analysis the base flow further decreased by the rate change of 0.026 m³/s. Similarly, the land cover change during 2015 was due to increment of agriculture land by 88 %.

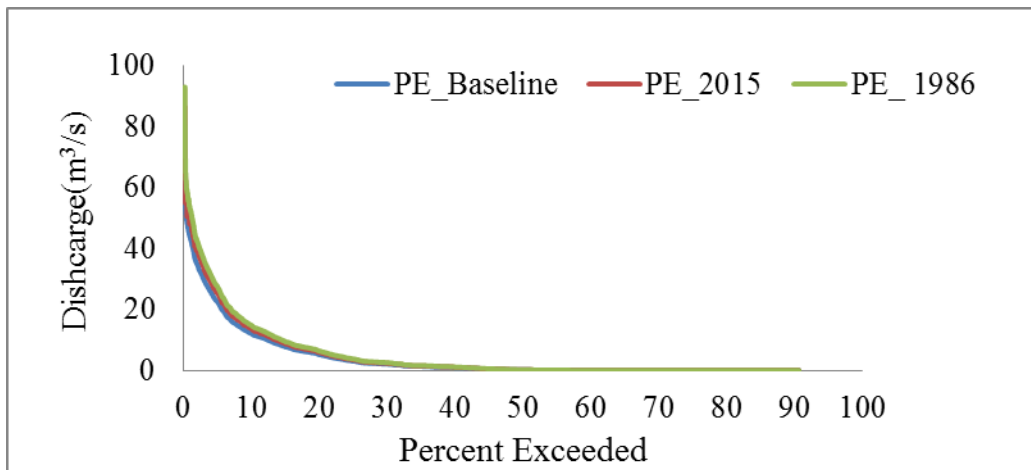


Figure 4.37 Flow Duration curves of observed low flow and using baseline, 1986 and 2015 land cover in Megech watershed

Currently there is a government program called afforestation different land cover of the watershed in order to preserve further change on the forest and that mainly by eucalyptus plantation trees. Researches done in upper Blue Nile basin reported that the observed increased afforested area did not improve the hydrological balance in watersheds because most of the eucalyptus trees planted is known to absorb a great amount of water. According to Maidment (1993), eucalyptus and pine types cause an average change of 40mm in annual flow for a 10% change in cover, with respect to grasslands in a correlation of inverse proportion. This means that a 10% increase in tree cover causes a decrease of annual flow by 40mm and vice versa.

Generally, hydrological investigation with respect to land cover change within Megech watershed showed that the river flow regimes have changed, with increases in peaks and reduction in base flows throughout the selected period of study. Some nine years ago the old Megech River (Photo 4.35 left) changed its course and currently passes through Robit village. For the purposes of the present study, the new course is referred to as the new Megech.



Figure 4.38: The Old (left) and New (right) Megech river pathways (Picture taken by Zemenu A.2015)

CHAPTER FIVE

5. CONCLUSION AND RECOMMENDATION

5.1 Conclusion

For the Megech watershed for the period (1973–2015) changes of land cover effect on the hydrological regime were analyzed. For assessing the changes in land cover we used three remote sensing images that were in the for the years (1973, 1986, 2015). An accuracy assessment by use of a confusion matrix for the supervised land cover classification indicates that the classification results are reliable. Land cover changes in the study area are assessed by post classification comparison were results showed that forest land decreased from 56 % in 1973 to 35 % in 1986. Agricultural land increased from 21 % in 1973 to 29 % in 1986. In the time period 1986–2015 forest land decreased from 35 % to 0.27 % while agricultural land increased from 29 % to 87 %. This indicates that the rate of deforestation is very high in the year of (1986-2015) as compared to the (1973-1986). The expansion of agricultural land in the period 1986–2015 is larger than in the previous time period suggesting that the demand for agricultural lands has increased

Performance of the model for both the calibration and validation catchment were found to be reasonably $NS=0.70$ and $NS=0.69$ for the calibration and validation respectively. Therefore HBV-96 model can be used or suitable for predicting the rainfall-runoff relationships as well as simulating discharge in the Megech watershed and was used for evaluating the impact of land cover change in the watershed.

Using 1986 land cover in the wet season, rainfall was peak, and a large amount of the stream flow generated from surface runoff. For the wettest months, flow records for the period (1987-1995), showed that the stream flow fluctuated between (9-37) percent of the annual flow compared with baseline land cover simulated stream flow. The maximum and minimum wet season flow records were 48% in 1995 and 8% in 1987 respectively.

Using the 2015 land cover, high flow analysis showed the stream flow further increased by the rate of change is $0.052 \text{ m}^3/\text{s}$, where as in the low flow analysis further decreased by the rate of change of $0.026 \text{ m}^3/\text{s}$. Similarly, the land cover change during this period was due to increase by the expansion of the

agriculture up to 88 %.The result showed that an increasing of the peak flow by 0.024 m³/s during the period of 1986-2015 and a decreasing of the base flow by the rate of change of 0.08m³/s.The indicates there will be Flooding in the watershed outlet area and drying of small streams during the dry season. This will affect the lively hood of the community living in the parts of watershed. As a result anew water management and utilization scenario has to be in place for sustainable use of the natural resource.

5.2 Recommendation

Similar studies in other watershed of the Blue Nile Basin can use this methodology and can improve study by using higher resolution of land sat images and more meteorological stations for improving model performance.

Built up area and agriculture land expansion are the major factors behind the land cover changes observed in the area. This finding highlights the need for comprehensive assessment of human activities and adaptation of sustainable forest management practices such as close supervision of forest reserves and making more closure lands available through restoration of already degraded lands.

IJSER

REFERENCES

- Agarwal, C, Green, G. M., Grove, J. M., Evans, T. P., and Schweik, C. M.City.Int. J (1927). Remote Sens. 23, .Climates.J.Hydrol, 238:231– 247Conference Applied Geologic Remote Sensing, 1–3 March 1999. Ann Arbor, MI: ERIM, II,
- Allen, R. (1998).Crop Evapotranspiration: Guidelines for computing crop water requirements. FAO, Rome.
- Alphan, H. (2003).Land-use change and urbanization of Adana, Turkey.LandDegrad.Dev.14, 575.Analysesfor regional hydrological modeling in the drainage basin. Hydrology WRP, Andgumara WRP,and gumara catchments
- Anderson, J.R., Hardy, E.E., Roach, T.J., Whitmer, R.E,(1976). A land use and land cover classification System for Use with Remote Sensor Data. Geological Survey Professional Paper No. 964, Washington,.
- Ashenafi, S. (2007).Catchment modelling and preliminary application of isotopes for model balance.Validation in upper Blue Nile Basin, Lake Tana, Ethiopia. UNESCO-IHE

- Bergström, S., Carlsson, B., Grahn, G. and Johansson, B.,(1997). A more consistent approach to catchment response in the HBV model.
- Besrgestrom.S. (1976) development and application of a conceptual runoff model
- Beven, G. V., (2000): Comparison of lumped and complex physical hydrological models, *Journal of Hydrology*, 133, 17-40
- Bewket, W. (2003). Dynamics in land cover and its effect on stream flow in the chemoga water shed Blue Nile basin, Ethiopia. *Hydro. Processes*, Vol. 19, Issue 2, pp. 445-458.
- Calder, I. (2002). Forests and hydrological services: reconciling public and science perceptions. *Land Use and Water Resources Research* 2, 2.1-2.12 (www.luwrr.com).
- Calder, R. (1995). The impact of land use change on water resources in sub-Saharan Africa: modeling study of Lake Malawi. *J. Hydrol*, 170, 123–135
- Campbell, J. B. (1983). *Mapping the land: Aerial imagery for land use information*. Washington, D.C.: Association of American Geographers.
- Campbell, J.B., (1996). Introduction to remote sensing. Chapters 10, pages 301-309 (A readable description of geometric correction). *Reanalysis Cartographic Reanalysis (CFRS)*, eco.web@tamu.edu
- Chow, V. T., David, R. M., and Larry, W. C. (1988). *Missed data treatment*, New York, PP, 145-171
- Colwell, R. (1983). *Manual of Remote Sensing*. American Society of Photogrammetric and Remote Sensing, 2nd edition. Falls Church, VA
- Croke, B.F.W. (2004). *A dynamic model for predicting hydrologic response to land covers*
D.editor. *World Soil Erosion and Conservation*. Cambridge Studies in Applied Ecology and Resource Management. Cambridge, UK: Cambridge University Press, pp 27–61.
- Coppin, P. & Bauer, M. (1996). *Digital Change Detection in Forest Ecosystems with Remote Sensing*.
- De Bruin, HAR, & Lablans, WN. (1998). Reference crop evapotranspiration determined with a modified Makkink equation. *Hydrological processes*, 12(7), 1053-1062.
- De Bruin, HAR, & Lablans, WN. (1998). Reference crop evapotranspiration determined with a modified Makkink equation. *Hydrological processes*, 12(7), 1053-1062.
- D. Tripathi and M. Kumar, (2012).“Remote Sensing Based Ana- lysis of Land Use/Land Cover Dynamics in Takula Block, Almora District(Uttarakhand),” *Journal of Human Ecol- ogy*, Vol. 38, No. , pp. 207-212

- EMA (Ethiopian Meteorological Agency).(1999). Meteorological Report of 1981. Addis Abeba, Ethiopia: Ethiopian, Meteorological Agency.
- Ephrem Alemu (2011). Effects of watershed characteristics on River flow for the case of Ribb
- Flugel, L. A. (1995). Delineating hydrological response units by geographical information system
- Gahegan, M. and Flack, J. (1999). The integration of scene understanding within a geographic information system: a prototype approach for agricultural applications. *Transactions in GIS*, 3, 31–49
- Goetz, A.F.H., Mckintosh, P.J., and Leslak, L.R. (1999). Multiyear calibration of Landsat TM for in studies of land use and land use change in the high plains. In: *Proceedings 13 International Conference Applied Geologic Remote Sensing*, 1–3 March 1999. Ann Arbor, MI: ERIM, II,
- Goetz, A.F.H., Mckintosh, P.J., and Leslak, L.R. (1999). Multiyear calibration of Landsat TM for studies of land use and land use change in the high plains. In: *Proceedings 13 International Conference Applied Geologic Remote Sensing*, 1–3 March 1999. Ann Arbor, MI: ERIM, II, p. 183.
- Goswami, Bhupendra Nath, Venugopal, V, Sengupta, D, Madhusoodanan, MS, & Xavier, Prince K. (2006). Increasing trend of extreme rain events over India in a warming environment. *Science*, 314(5804), 1442-1445.
- Gupta, Rajiv, Mehofer, Eduard, & Zhang, Youtao. (2002). Profile guided compiler optimizations.
- Habtom .M, (2009). Evaluation of climate change impact on upper Blue Nile Basin.
- Hargreaves, George H, & Samani, Zohrab A. (1982). Estimating potential evapotranspiration. *Journal of the Irrigation and Drainage Division*, 108(3), 225-230.
- Hargreaves, George H, & Samani, Zohrab A. (1982). Estimating potential evapotranspiration. *Journal of the Irrigation and Drainage Division*, 108(3), 225-230.
- Hashiba, H., Kameda, K., Uesugi, S., and Tanaka, S. (2000). Land use change analysis of Tama River Basin with different spatial resolution sensor data by Landsat/MSS and TM. *Adv. Space Res.* 26, 1069
- Herold, M. (2003). The spatiotemporal form of urban growth: Measurement, analysis and modeling. *Remote Sens. Environ.* 6, 286
- Huete A.R. and C.J. Tucker (1991). Investigation of soil influences in AVHRR red and near- infrared vegetation index imagery. *International Journal of Remote Sensing* 12, 6: 1223-1242 Changes in gauged and ungauged catchments. *J. Hydrol*, 291, 115–131.

- Hurni, H. (1993). Land degradation, famine, and land resource scenarios in Ethiopia. In: Pimentel IIASA, Laxenburg, Austria, 22 pp. [Available from International Institute for Applied Imagery. Remote Sensing Reviews. Vol. 13. P.207. -234P.207-234.
- J. R. Jensen,(2005). "Introductory Digital Image Processing: A Remote Sensing Perspective," In: K. C. Clarke, Ed., 3rd Edition, Prentice Hall, The United States of America,.
- Kardoulas, N.G., Bird, A.C., and Lawan, A.I., (1996). Geometric correction of SPOT and Landsat imagery: a comparison of map and GPS-derived control points. Photogrammetric Engineering and Remote Sensing, 62, 1173-1177.
- Kahsay, B.Kassay, B.(2004). Land use and land cover change in central high lands of Ethiopia. MScresearch paper, Addis Ababa University
- Legesse, D. (2003). Hydrological response of a catchment to climate and land use changes in tropical Africa: case study South Central Ethiopia. T. Hydrol, 275, 67-85
- Liden, R. (2000) Analysis of conceptual rainfall-runoff modeling performance in Different climates. J.Hydrol, 238:231– 247.
- Lillesand, T.M., and Kiefer, R.W.,(2000). Remote sensing and image interpretation. Chapter 7, pages 473-477 (A very short general coverage).
- Lillesand, T. and R. Kiefer. (2004). Remote Sensing and Image Interpretation. Fifth Edition. John Wiley & Sons, Inc, New York
- Lindstrom, G. (1997). Development and test of the distributed HBV-96 hydrological model.
- Macleod and Congalton. 1998. A Quantitative Comparison of Change Detection Algorithms for Monitoring Eelgrass from Remotely Sensed Data. Photogrammetric Engineering & Remote Sensing. Vol. 64. No. 3. p. 207 - 216.
- Maidment, D.R. (1993). Hand book of hydrology, McGraw – Hill, New York, pp.113.
- Maingi, J.K. (2001). Assessment of environmental impacts of river basin development on the riverine forests of eastern Kenya using multi-temporal satellite data. International Journal of Remote Sensing, 22(14):2701-2729
- Mather, P.M., (1995). Map-image registration using least–squares polynomials. International Journal of Geographical Information Systems, 9, 543-554.
- Mather, P.M., (1999). Computer processing of remotely-sensed images. Chapter 4, pages 75-87 (Excellent readable coverage, including orbital geometry models not covered in the lecture.).

- Melesse, Assefa M, Abtew, Wossenu, & Dessalegne, Tibebe. (2009). Evaporation estimation of Rift Valley Lakes: comparison of models. *Sensors*, 9(12), 9603-9615.
- Meyer, W.B. and Turner, B.L. II, editors. (1994). Changes in land use and Land cover: A Global
- Mitiku Haile, (2006): Sustainable Land Management – A New Approach to Soil and Water Conservation in Ethiopia (T. H. M. Rientjes¹, B. U. J. Perera², A. T. Haile¹, P. Reggiani³, and L. P. Muthuwatta) modeling. *Remote Sens. Environ.* 6, 286. modelling Modelling study of Lake Malawi. *J. Hydrol*, 170, 123–135. models. In: Abbott, M.B., Refsgaard, J.C. (Eds.), Distributed Hydrological Modeling research paper, Addis Ababa University.
- Moges, SA, Katambara, Z, & Bashar, K. (2003). Decision support system for estimation of potential evapotranspiration in Pangani Basin. *Physics and Chemistry of the Earth, Parts A/B/C*, 28(20), 927-934.
- Monserud, R. A., (1990): Methods for comparing global vegetation maps. Working Paper WP-90-40,
- Monserud, Robert A, & Leemans, Rik. (1992). Comparing global vegetation maps with the Kappa statistic. *Ecological Modelling*, 62(4), 275-293.
- Morad, M., Chalmers, A.I., and O, Regan, P.R., (1996). The role of root mean square error in the geotransformation of images in GIS. *International Journal of Geographical Information Systems*, 10, 347-353.
- Moshen A. (1999). Environmental Land Use Change Detection and Assessment Using with Multi – temporal Satellite Imagery. Zanzan University.
- Nash, J.E., and Sutcliffe, J.V. (1970). River flow forecasting through conceptual models part I—A discussion of principles. *Journal of hydrology*, 10(3), 282-290.
- National Aeronautics and Space Administration (2001). The Landsat Program. Retrieved June 3, 2001, from <http://landsat.gsfc.nasa.gov>
- Parkin, G. (1996). Validation of catchment models for predicting land-use and climate Pp.181-109 Pp.181-109.
- Priestley, CHB, & Taylor, RJ. (1972). On the assessment of surface heat flux and evaporation using large-scale parameters. *Monthly weather review*, 100(2), 81-92.
- Prol-Ledesma, R.M., Uribe-Alcantara, E.M., and Diaz-Molina, O. (2002). Use of cartographic data and Landsat TM images to determine land use change in the vicinity of México City. *Int. J. Remote Sens.* 23, 1927
- Refsgaard, J.C. (1996). Terminology, modeling protocol and classification of hydrological models. In: Abbott, M.B., Refsgaard, J.C. (Eds.), Distributed Hydrological Modeling Kluwer, Dordrecht, pp. 17–39.

- R. B. Thapa and Y. Murayama, (2009). "Urban Mapping, Accuracy, & Image Classification: A Comparison Multiple Approaches in Tsukuba City, Japan," *Applied Geography*, Vol. 29, No. , pp. 135-144
- Singh, A. (1989). Digital Change Detection Techniques Using Remotely Sensed Data. *International Journal of Remote Sensing*. Vol. 10, No. 6, p. 989-1003.
- Skakun, R., Franklin, S.E., and Wulder, M.A. (2003). Sensitivity of the EWDI to mountainpine beetle red-attack damage. *Remote Sensing of Environment*, 30, 433–443
- Temesegen and Melesse, (2013). A simple temperature method for the estimation of the National the National Centers for Environmental Prediction (NCEP) Climate Forecast SystemTM. *Adv. Space Res.* 26, 1069. tropical Africa: case study South Central Ethiopia. *T. Hydrol*, 275, 67-85.
- Tucker C., C. Vanparet, and A. Gaston. (1983). Satellite remote sensing of total dry matter production in the Senegalese Sahel. *Remote Sensing Environment* 17: 233-249
- Wale, A, Rientjes, THM, Gieske, ASM, & Getachew, HA. (2009). Ungauged catchment contributions to Lake Tana's water balance. *Hydrological processes*, 23(26), 3682-3693.

IJSER

Annexes

Appendix A: Meteorological Stations, percentage missing and double mass

Arithmetic Average Method used to fill missed data values which have percentage missing of less than 10% of the time. The method can keep variability of the data for stations with percentage missing value of less than or equal to 10% (Chow et al., 1988)

Table A.1 Meteorological stations and percentage missing (%)

Station Name	X	Y	Elevation	Area_Sqkm	Weight (%)	Period	Percentage of missing
Shermbekit	37.49	12.64	2460	379.36	0.82	1986-1995	9.27
Gonder	37.42	12.55	2083	119.8	0.18	1986-1995	7.1
Makesegnet	37.55	12.37	1930	0	0	0	0
Tikeledenegay	37.33	12.71	1829	0	0	0	0
Total				499.16	1	0	0

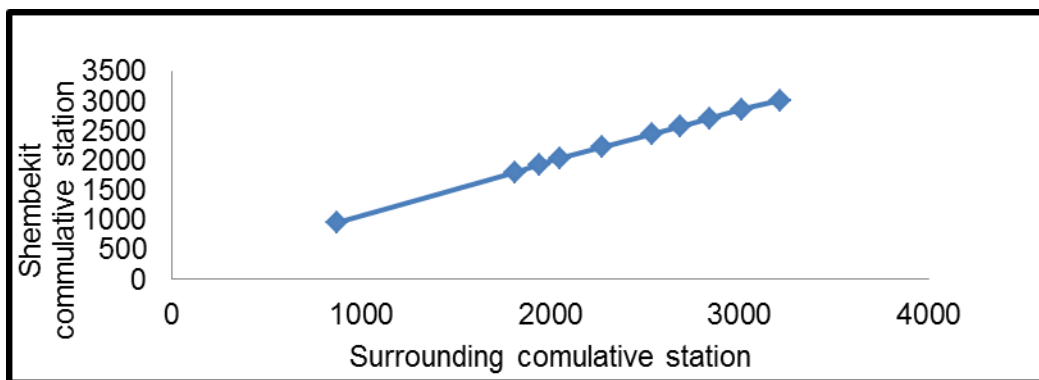


Figure A1 Double Mass Curve analysis

Table A.3: Average evapotranspiration using temperature (Enku and Melese, 2014)

Period	Monthly_Eto	1	2	3	4	5	6	7	8	9	10	11	12
1986-1995	Ave_E	3.01	3.07	3.28	3.2	2.88	2.12	1.69	1.78	2.17	2.52	3.08	3.1

1. Model efficiency

1.1 Nash-Sutcliffe efficiency E

The efficiency E proposed by Nash and Sutcliffe (1970) is defined as one minus the sum of the absolute squared differences between the predicted and observed values normalized by the variance of the observed values during the period under investigation. It is calculated as:

$$NS = 1 - \frac{\sum_{i=1}^N (Q_o - Q_s)^2}{\sum_{i=1}^N (Q_o - Q_o)^2}$$

Where, Q_o : Observed flow, Q_s : Simulated flow and Q_o : Average of observed flow

2.3. Model efficiency

$$RV_E = \left[\frac{\sum_i^n Q_{obs(i)} - \sum_i^n Q_{sim(i)}}{\sum_i^n Q_{obs(i)}} \right] * 100$$

2.4. Model efficiency

$$PBIAS = \left[\frac{\sum_i^n (Q_i^{obs} - Q_i^{sim}) * 100}{\sum_i^n (Q_i^{obs})} \right]$$

year	1986	2015	baseline
------	------	------	----------

Appendix B: Sensitivity Analysis of HBV model Parameters and Optimum Parameter Space

Table B.1: Sensitivity parameter

FC	NSE	RVE(%)	K4	NSE	RVE	khq	NSE	RVE(%)	Alpha	NSE	RVE(%)
400	0.6632	-17.37	0.036	0.7494	0.4805	0.07	0.77	2.162	0.18	0.7	-0.23
360	0.6891	-14.05	0.032	0.7531	0.477	0.08	0.756	1.978	0.3	0.69	-0.23
320	0.7132	-10.59	0.029	0.7567	0.4653	0.07	0.763	1.745	0.5	0.679	-0.23
280	0.7345	-7.024	0.025	0.7601	0.4573	0.06	0.769	1.432	0.7	0.66	-0.23
240	0.7525	-3.363	0.022	0.7631	0.4184	0.05	0.772	0.997	0.9	0.65	-0.23
200	0.7655	0.333	0.018	0.7655	0.333	0.05	0.766	0.333	1	0.64	-0.23
160	0.7728	4.019	0.014	0.7671	0.1454	0.04	0.739	-0.77	1.1	0.63	-0.23
120	0.7739	7.649	0.011	0.7674	-	0.03	0.666	-2.84			
110	0.7691	11.221	0.007	0.766	-	0.02	0.483	-7.62			
100	0.7586	14.92	0.004	0.7624	-	0.01	0.204	-13.2			
Lp	NSE	RVE	Perc	NSE	RVE	Beta	NSE	RVE			
0.08	0.7687	1.0052	0.6	0.765	0.2647	2.2	0.738	-0.98			
0.06	0.7677	0.7713	0.5	0.765	0.2647	1.98	0.742	-0.83			
0.044	0.7668	0.5902	0.42	0.765	0.259	1.76	0.747	-0.65			
0.032	0.7661	0.4545	0.38	0.765	0.256	1.54	0.752	-0.43			
0.024	0.7657	0.3701	0.34	0.765	0.254	1.32	0.758	-0.15			
0.02	0.7655	0.333	0.28	0.7655	0.333	1.1	0.766	0.333			
0.016	0.7653	0.2985	0.26	0.765	0.2526	0.88	0.775	0.861			
0.012	0.7651	0.2698	0.24	0.765	0.2529	0.66	0.786	1.753			
0.008	0.765	0.252	0.22	0.765	0.2546	0.44	0.799	3.315			
0.004	0.765	0.2511	0.2	0.7651	0.251	0.22	0.807	7.553			

Appedex C low flow

Table C1 :1Low flow data

1987	0.10	0.10	0.10
1988	0.10	0.10	0.10
1989	0.10	0.10	0.10
1990	0.20	0.20	0.11
1991	0.09	0.10	0.10
1992	0.06	0.06	0.06
1993	0.08	0.08	0.06
1994	0.29	0.30	0.06
1995	0.12	0.11	0.06

Table C3: Annual Maximum Stream flow

year	Maximum flow		
	baseline	1986	2015
1987	47	39	48
1988	42	46	46
1989	45	39	41
1990	53	57	53
1991	55	58	47
1992	52	47	48
1993	45	45	45
1994	60	47	57
1995	129	133	135

TableTableC4: Total Stream Flow

year	Total stream flow		
	baseline	1986	2015
1987	1329	1390	1214
1988	1567	1858	1653
1989	1034	1084	960
1990	1550	1685	1598
1991	801	1074	855
1992	1097	904	756
1993	1265	1144	1161
1994	1099	1133	1176

1995	1113	1172	1224
------	------	------	------

Appendix D: Locations of Ground Control points in the Study Area

Table D1: GCP

ID	X	Y	Type of land cover
1	338745.14	1394366.46	Agriculture
2	338318.53	1394696.92	Agriculture
3	333201.28	1394489.69	Built up area
4	329268.06	1388680.26	Built up area
5	328875.16	1389278.09	Agriculture
6	331672.69	1393270.08	Built up area
7	336032.24	1395074.06	Forest
8	335681.11	1395376.56	water
9	335140.33	1395815.9	Forest
10	336714.25	1394954.96	Agriculture
11	336077.09	1395930.3	Forest
12	334837.7	1394923.23	Built
13	333276.15	1396754.23	Forest
14	332542.24	1398323.85	Forest
15	333712.15	1399418.69	Agriculture
16	335833.05	1395264.92	water
17	336412.64	1395311.24	Agriculture
18	336228.13	1395486.21	Agriculture
19	336283.45	1395355.47	Agriculture
20	336381.16	1395439.32	Forest
21	336158.45	1395643.57	Agriculture
22	336106.47	1395885.8	Forest
23	336563.62	1395627.7	Agriculture
24	336634.85	1395582.31	Forest
25	336557.79	1395537.3	Agriculture
26	336610.43	1395211.51	Agriculture
27	336651.28	1395302.1	Agriculture
28	336386.81	1395197.8	Agriculture
29	336453.43	1395262.87	Forest

ID	X	Y	Type of land cover
51	335992.87	1405483.95	Agriculture
52	336020.16	1405393.49	Forest
53	336108.64	1405281.82	Agriculture
54	336110.37	1405251.46	Agriculture
55	336109.57	1405173.89	Agriculture
56	336165.32	1405079.11	Forest
57	336198.35	1405036.13	Forest
58	336208.91	1405015.55	Agriculture
59	336270.72	1405020.03	Agriculture
60	336334.86	1405024.62	Agriculture
61	336377.14	1404978.45	Agriculture
62	336417.84	1404933.13	Forest
63	336464.51	1404890.57	Forest
64	336469.18	1404793.74	Forest
65	336550.14	1404750.44	Forest
66	336655.57	1404639.16	Agriculture
67	336739.29	1404652.04	Agriculture
68	336810.13	1404656.94	Agriculture
69	336833.64	1404567.79	Agriculture
70	336928.04	336928.04	Built
71	337002.13	1404577.35	Agriculture
72	337045.34	1404475.76	Agriculture
73	337124.41	1404400.66	Agriculture
74	337181.54	1404387.08	Agriculture
75	337220.17	1404308.07	Agriculture
76	337290.77	1404220.98	Built
77	337288.09	1404116.44	Forest
78	337357.72	1404120.01	Forest
79	337361.64	1404034.67	Forest

30	334037.2	1394733.52	Built
31	333391.02	1394775.01	Built
32	333484.62	1394475.27	Built
33	333759.84	1394786.17	Built
34	333601.53	1394798.16	Built
35	334339.93	1398520.24	Agriculture
36	334934.66	1398313.75	Agriculture
37	334716.27	1398133.38	Built
38	332704.45	1398389.95	Forest
39	335223.54	1396224.29	water
40	335659.17	1406459.35	Agriculture
41	335663.88	1406173.42	Agriculture
42	335661.94	1406114.71	Agriculture
43	335865.41	1406255.23	Forest
44	335661.73	1406022.55	Agriculture
45	335659.74	1405833.16	Forest
46	335752.75	1405738.43	Forest
47	335748.88	1405680.08	Agriculture
48	335814.17	1405651.87	Forest
49	335841.12	1405581.52	Forest
50	335926.67	1405483.13	Agriculture

80	337421.09	1404030.31	Agriculture
81	337459.32	1403922.98	Agriculture
82	337534.13	1403854.65	Forest
83	337547.77	1403616.14	Agriculture
84	337549.79	1403418.58	Agriculture
85	337549.07	1403270.56	Forest
86	337616.19	1403202.86	Agriculture
87	337674.63	1403216.72	Forest
88	337727.36	1403185.78	Agriculture
89	337779.67	1403108.41	Agriculture
90	337804.13	1403054.58	Forest
91	337884.22	1403014.86	Forest
92	337920.93	1402942	Agriculture
93	337990.66	1402880.97	Agriculture
94	338108.14	1402758.95	Forest
95	338177.61	1402594.85	Forest
96	338213.66	1402588.75	Agriculture
97	338347.45	1402577.41	Forest
98	338404.58	1402431.87	Forest
99	338362.82	1402312.71	Forest
100	338312.2	1402234.6	Forest

IJSER